The Abdus Salam International Centre for Theoretical Physics

United Nations Educational, Scientific and Cultural Organization

IAEA International Atomic Energy Agency

1936-37

Advanced School on Synchrotron and Free Electron Laser Sources and their Multidisciplinary Applications

7 - 25 April 2008

Multiple Scattering approach to X-Ray Absorption Spectroscopy

M. Benfatto
Laboratori Nazionali di Frascati dell'INFN
Frascati
ITALY

Multiple Scattering approach to X-Ray Absorption Spectroscopy

M. Benfatto

Laboratori Nazionali di Frascati dell'INFN – Frascati ITALY

Plan of these lessons

- **MS Theory**

  Generalities
  Muffin-Tin approximation
  Problems and prospectives

- **XAS spectroscopy**

  Examples

- **Quantitative analysis of the XANES energy region**

  Method and examples

MS Theory

- **It is a method to solve the Sch. Equation in real space** - It has been developed by K. H. Johnson since '60-'70

$$\left[-\nabla^2 + V(\vec{r})\right]\Psi(\vec{r}) = E\Psi(\vec{r})$$

$$V(\vec{r}) = V_c(\vec{r}) + V_{exc}(\vec{r})$$

one -electron

$$V_c(\vec{r}) = \sum_j V^j(\vec{r} - R_j)$$

$$V_{exc}(\vec{r}) = -6\alpha\left[\frac{3}{8\pi}\rho(\vec{r})\right]^{1/3}$$

$$V_c(\vec{r}) = \sum_j V^j(\vec{r} - R_j)$$

Sum of free atom potential ⟷ cluster of atoms

Muffin-Tin approximation

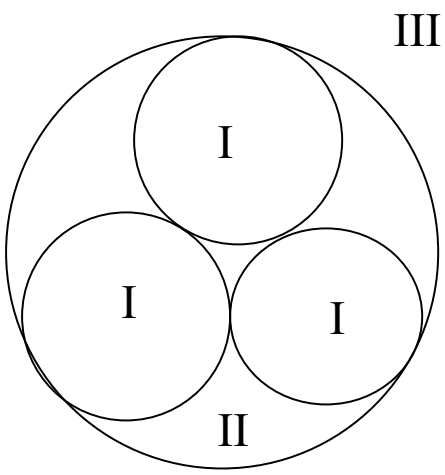

The space is divided in three regions

I region

$$V_I(\vec{r}) = \sum_L V_L(r) Y_L(\hat{r}) \; ; L \equiv l, m$$

Only the L=0 is considered

II region

$$V_{II}(\vec{r}) = V_{MT} = \frac{1}{\Omega_{II}} \int_{\Omega_{II}} V(\vec{r})\, d\vec{r}$$

V_{MT} is a constant value
The average is over the interstial volume

III region

V_{III} is a spherical average respect respect to the atomic cluster center
It depends to the physical problem to be solved.

We must solve the Sch. equation with this potential

The total w.f. can be written as:

$$\Psi = \sum_i \Psi_I + \Psi_{II} + \Psi_{III}$$

- In each atomic region (region I) the w.f. is developed into spherical harmonics:

$$\Psi_I^J(\vec{r}) = \sum_L B_L^J R_l^J(E;r) Y_{lm}(\hat{r})$$

- V_{MT} is constant $\longrightarrow \Psi_{II}$ is a combination of Bessel and Neumann functions

In the outer sphere region (region III)

$$\Psi_{III} = \sum_{L,L'} [A_L^{III} f_l^{III}(kr_0)\delta_{LL'} + B_{LL'}^{III} g_{l'}^{III}(kr_0)] Y_{L'}(\hat{r}_0)$$

regular part

center of the whole molecules

irregular part

This is a very general expression - The asymptotic behavior of f_l and g_l allow us to go from bound to continuum states.

We impose the continuity of wave function Ψ and its first derivate at the border of the different regions

$\Downarrow$

Compatibility equations between B_L^j coefficients

$\Downarrow$

i) Eigen-values of the bounded molecular states
ii) w.f. in the various regions
iii) Spectroscopy quantities

Starting from the Lippmann-Schwinger equation and using the Green's theorem, we derive

$$B_L^i(\underline{L}) + t_l^i \sum_{j \neq i} \tilde{G}_{LL'}^{ij} B_{L'}^j(\underline{L}) = -\, t_l^i J_{L\underline{L}}^{io} \Gamma_{\underline{L}}$$

valid for both bound and continuum states

$$\tilde{G}_{LL'}^{ij} = G_{LL'}^{ij} - \sum_{L''} J_{LL''}^{i0} t_{l''}^{0} J_{L''L'}^{oj}$$

corrections due to the OS sphere, region III

$$t_l^i = e^{i\delta_l^i} \sin \delta_l^i$$

$$G_{LL'}^{ij} = -4\pi i \sum_{L''} i^{l''+l'-l} C_{L'L''}^{L} h_{l''}^{+}(kR_{ij}) Y_{L''}(\hat{R}_{ij})$$

$$G_{LL'}^{ii} \equiv 0$$

$$J_{L\underline{L}}^{i0}$$

Gaunt coefficient

Exciting wave referred to site i

$$B_L^i(\underline{L}) + t_l^i \sum_{j \neq i} \widetilde{G}_{LL'}^{ij} B_{L'}^j(\underline{L}) = -t_l^i J_{L\underline{L}}^{io} \Gamma_{\underline{L}}$$

The amplitude of the wave function at each atomic site i is formed by the one coming from the center plus all arriving from the other sites.

The model is a multiple scattering model for several centers with free propagation in the interstitial region

Bound states

$$\sum_{j,L'} [T_a^{-1} + \widetilde{G}]_{L,L'}^{ij} B_{L'}^j(\underline{L}) = \sum_{j,L'} [M - i\Delta]_{L,L'}^{ij} B_{L'}^j(\underline{L}) = J_{L,\underline{L}}^{i0} \Gamma_{\underline{L}}$$

$$(T_a^{-1})_{L,L'}^{ij} = [(t_l^i)^{-1}] \delta_{ij} \delta_{L,L'}$$

where

$$M^{ij}_{L,L'} = \cot(\delta^{i}_{l})\delta_{ij}\delta_{L,L'} + (1-\delta_{ij})N^{ij}_{L,L'} + \sum_{L''} J^{i0}_{L,L''}\alpha^{0}_{l''}J^{0j}_{L'',L'}$$

$$\Delta^{ij}_{L,L'} = \frac{\pi}{\sqrt{E-V_0}}\sum_{\underline{L}} J^{i0}_{L,\underline{L}}\Gamma_{\underline{L}}\Gamma^{*}_{\underline{L}}J^{0j}_{\underline{L},L'}$$

imposing as boundary condition in the region III the exponential decay of the wave function, we find

$$\Gamma_{\underline{L}} = 0$$

$$\sum_{j,L'}[T_a^{-1}+\tilde{G}]^{ij}_{L,L'}B^{j}_{L'}(\underline{L}) = \sum_{j,L'}[M]^{ij}_{L,L'}B^{j}_{L'}(\underline{L}) = 0$$

$$\downarrow$$

$$Det[M(E)] = 0$$

Condition for nontrivial solutions - it gives us the energy levels of the bound states in the negative real energy axis

MnO_4^- T_d symmetry

Keith H. Johnson

TABLE I

SCF–Xα Electronic Energy Levels (in Rydbergs) of an MnO_4^- Cluster in a Crystalline Environment[a]

Symmetry	Energy Levels
$7a_1$	−0.006
$8t_2$	−0.020
$7t_2$	−0.350
$2e$	−0.526
$1t_1$	−0.682
$6t_2$	−0.761
$6a_1$	−0.775
$1e$	−0.901
$5t_2$	−0.915
$4t_2$ (O 2s)	−1.785 (−1.732)
$5a_1$ (O 2s)	−1.813 (−1.732)
$3t_2$ (Mn 3p)	−4.259 (−3.952)
$4a_1$ (Mn 3s)	−6.435 (−6.126)
$2t_2$ (O 1s)	−37.738 (−37.822)
$3a_1$ (O 1s)	−37.738 (−37.822)
$1t_2$ (Mn 2p)	−46.513 (−46.274)
$2a_1$ (Mn 2s)	−54.105 (−53.859)
$1a_1$ (Mn 1s)	−468.584 (−468.203)

Empty levels

Core states

[a] Levels below the dashed line are fully occupied in the ground state; those above the line are empty. Corresponding "free-atom" energy levels are shown in parentheses.

TABLE IV

Theoretical and Experimental Optical Transition Energies (in eV) for MnO_4^-

Transition	Unrelaxed SCF calculation	Transition-state calculation	Experiment[a]
$1t_1 \rightarrow 2e$	2.1	2.3	2.3
$6t_2 \rightarrow 2e$	3.2	3.3	3.5
$1t_1 \rightarrow 7t_2$	4.5	4.7	4.0
$5t_2 \rightarrow 2e$	5.3	5.3	5.5

[a] See Holt and Ballhausen (1967).

continuum states

$$B^i_L(\underline{L}) + t^i_l \sum_{j \neq i} \widetilde{G}^{ij}_{LL'} B^j_{L'}(\underline{L}) = -\, t^i_l J^{io}_{L\underline{L}} \Gamma_{\underline{L}}$$

$$\sum_{j,L'} [M - i\Delta]^{ij}_{L,L'} B^j_{L'}(\underline{L}) = J^{i0}_{L,\underline{L}} \Gamma_{\underline{L}}$$

we want to find the conditions to have continuum resonances, i.e. sharp increase of the amplitude B^j_L

$$B^i_L \propto [(I - iM^{-1}\Delta)^{-1} M^{-1}\Delta]^{ii}_{L.\underline{L}}$$

$$Det\, M[E] = 0$$

we have resonance at the energies where the above relation holds - it is the same condition to find bound states - bound states at negative energies while here we are at positive energies

This relation indicates that bound states can be found as continuum resonance if we can go to negative energies in the continuum calculation - the matrix M is the same

we must eliminate the OS - the potential at the infinite is V_{MT}

$$\tilde{G}^{ij}_{LL'} = G^{ij}_{LL'}$$

$$\sum_{j,L'} [T_a^{-1} + G]^{ij}_{L,L'} B^j_{L'}(\underline{L}) = \sum_{j,L'} [M_o - i\Delta]^{ij}_{L,L'} B^j_{L'}(\underline{L}) = J^{i0}_{L,\underline{L}}$$

$$(M_o)^{ij}_{L,L'} = \cot(\delta^i_l)\delta_{ij}\delta_{L,L'} + (1-\delta_{ij}) N^{ij}_{L,L'}$$

but $M_o \approx M$ for energies E such that $E - V_{MT} > 0$

they have almost the same poles

In other words for $E > V_{MT}$ (it is a negative value) we can found all the possible states as continuum states (in a one electron picture)

“extended continuum” scheme

We can calibrate on the same energy scale the bound state features relative to the continuum features without the need to perform ionization energy calculation

unique energy scale of the pre-edge energy region with the rest of the XAS spectrum.

S. Doniach et al. Proceedings of “EXAFS and Near Edge Structure III” Stanford (1984)
M. Benfatto et al. Phys. Rev B (1986)
T. Tyson et al. Phys. Rev B (1992)

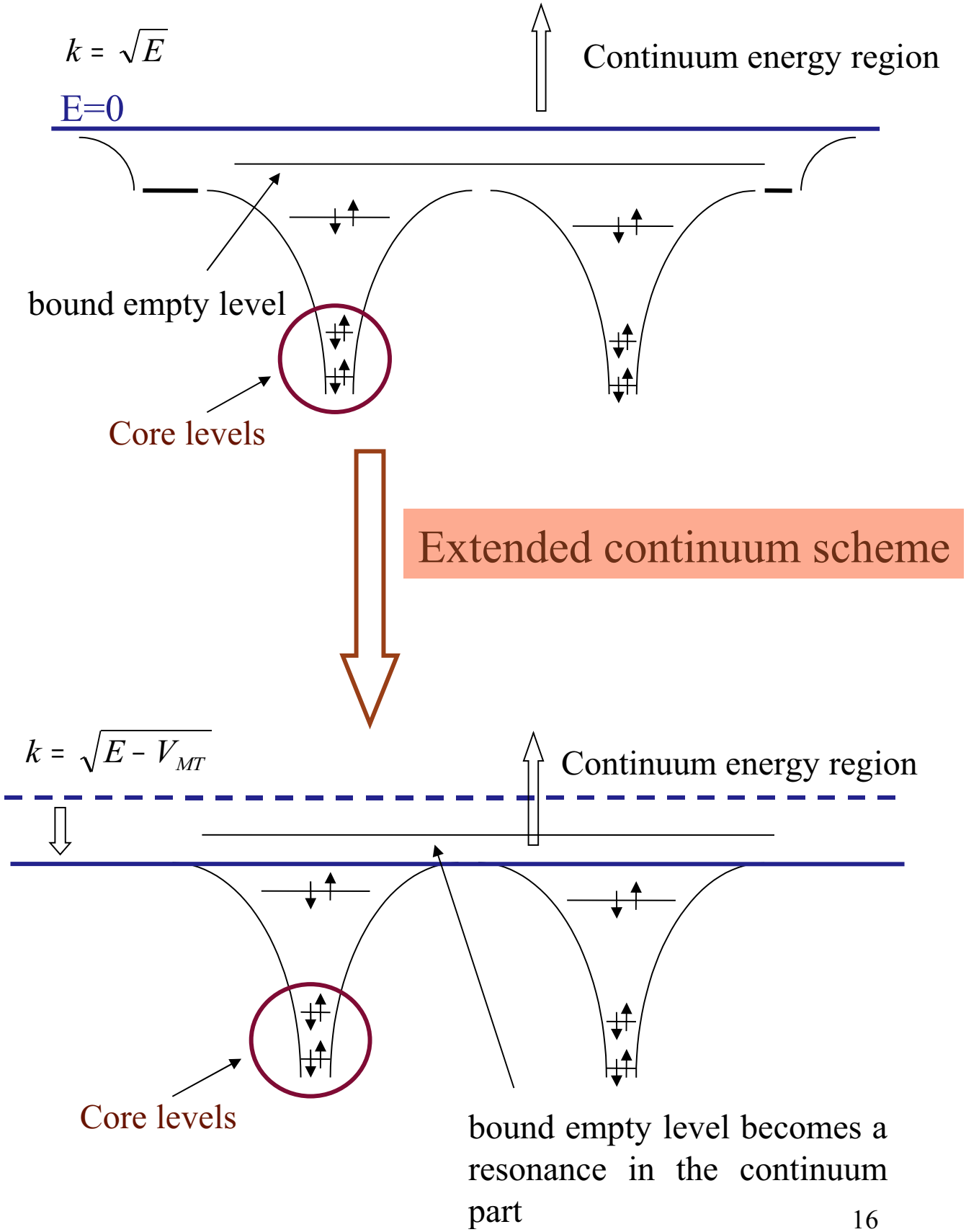
$k = \sqrt{E}$
Continuum energy region
E=0
bound empty level
Core levels
Extended continuum scheme
$k = \sqrt{E - V_{MT}}$
Continuum energy region
Core levels
bound empty level becomes a resonance in the continuum part

Absorption coefficient from core levels

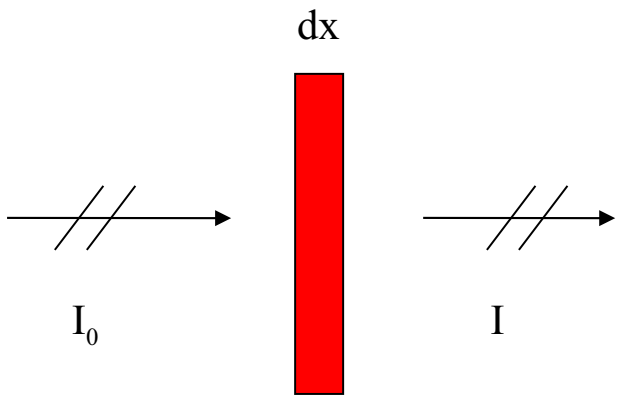

$$dI=\mu(E)\, I\, dx \longrightarrow I=I_0 e^{-\mu(E)x}$$

$$\mu(E) = n_{ab}\, \sigma(E)$$

E is in the X-ray energy range

Density of absorption medium

Photoabsorption cross section

There are other scattering processes
with and without energy loss

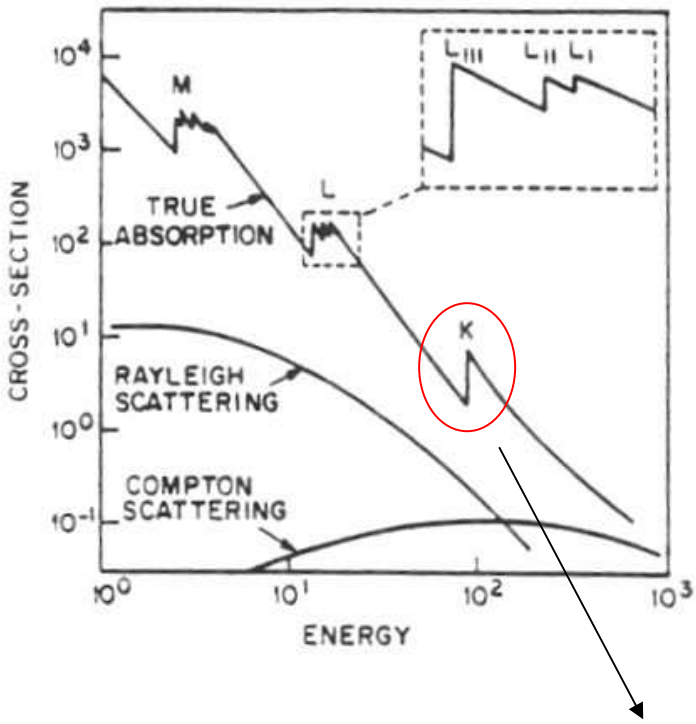

iodine

33 KeV

The photoabsorption process dominates

$K = 1s \longrightarrow \varepsilon p$; $L_I = 2s \longrightarrow \varepsilon p$ .....

Every atomic species has a well defined edges
It is possible to select the species and its environment

Structural and electronic information on the absorbing site from the strong oscillations with energy $\longrightarrow$ XAFS

Physical process: excitation of core-level electron to continuum states

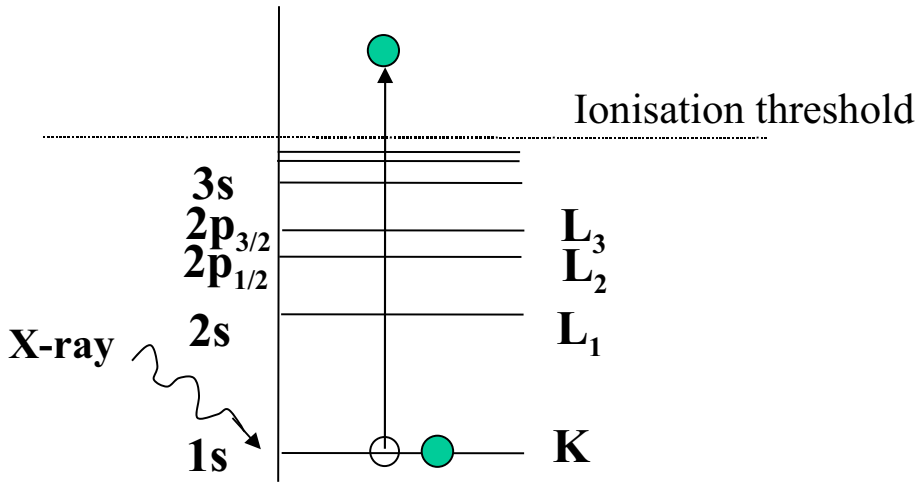

We use the Fermi "golden rule" to calculate the total cross-section of this process

The photoabsorption cross section is defined through the Fermi "golden rule"

$$\sigma(\omega) = 4\pi^2 \alpha\, \omega \sum_f \left| \langle \psi_f | \vec{\varepsilon} \cdot \vec{r} | \psi_c \rangle \right|^2 \delta(\omega - E_f + E_c)$$

$$\alpha = \frac{1}{137}$$ Fine structure constant

Dipole approximation $\longleftrightarrow$ $\dfrac{\sigma_q(\omega)}{\sigma_d(\omega)} \approx \dfrac{1}{100}$

$\psi_f \longrightarrow$ continuum part of the w.f.

$\psi_c \longrightarrow$ core w.f. spatially localized

We need to know the final state wave function at site 0 because of the localization of the core wave function

$$\sigma(\omega) = A(\omega) \sum_{\underline{L},L,m_\gamma,m_0} \left|B_L^0(\underline{L})\right|^2 \left|(R_L^0(\vec{r}_0)\,|\,r_0 Y_{lm_\gamma}(\hat{r}_0)\,|\,\phi_{l_0}(r_0) Y_{L_0}(\hat{r}_0))\right|^2$$

$$A(\omega) = 2\pi\alpha\omega\,(4\pi/3)^2 \frac{k}{\pi} \qquad \begin{cases} k = \sqrt{E - V_{MT}} \\ E = \omega - I_0 \end{cases}$$

un-polarized photo-absorption cross section

Energies k^2 are measured in Rydbergs (1 Ry = 13.60529 eV) and lengths in Bohrs.

Optical theorem

$$\sum_{\underline{L}} [B^0_L(\underline{L})]^* [B^0_{L'}(\underline{L})] = \mathrm{Im}[(I - T_a G)^{-1} T_a]^{00}_{LL'}$$

$$\tau^{00}_{LL'} = [(I - T_a G)^{-1} T_a]^{00}_{LL'}$$

$$\begin{pmatrix} .. & & G_{ij} \\ & (t^i_\ell)^{-1} & \\ G_{ji} & & .. \end{pmatrix}^{-1}$$

scattering path operator – it contains all the structural and electronic information

complete equivalence between band structure,Green function and MS approach

Photoabsorption cross section

$$\sigma(E) = (l+1)\sigma_0^{l+1}(E)\chi^{l+1}(E) + l\sigma_0^{l-1}(E)\chi^{l-1}(E)$$

$$\chi^{l}(E) = \frac{1}{(2l+1)\sin^2\delta_l^0}\sum_m \mathrm{Im}\,\tau_{lmlm}^{00}$$

$$\sigma_0^l(E) = \frac{8\pi^2}{3}\alpha\, k(E+I_0)\sin^2\delta_l^0\left[\int_0^\infty r^3 R_l(r)\phi_{l_0}(r)\,dr\right]^2$$

atomic cross section - almost without structures and independed from the energy

Final angular momentum according dipole selection rule

$$l = l_0 \pm 1$$

The scattering path operator can be calculated exactly or by series when the spectral radius ρ less than one

$$\tau^{00}_{LL'} = [(I - T_a G)^{-1} T_a]^{00}_{LL'}$$

$$(I - T_a G)^{-1} = \sum_{n=0} (T_a G)^n$$

$$\tau = T_a + T_a G T_a G T_a + T_a G T_a G T_a G T_a + \ldots..$$

$$G^{ii}_{LL'} \equiv 0$$ we start from n=2

The size of the spectral radius depends by the energy

MS paths

$$\sigma_n = \sigma_0 \chi_n^l$$

σ_0 – smooth atomic contribution

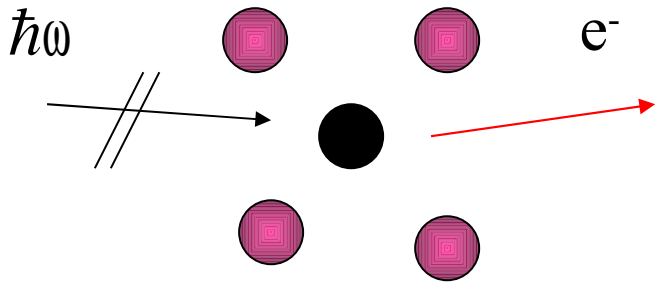

σ_2 – single diffusion – EXAFS region

$$t_l^0 G\, t_l^i G\, t_l^0$$

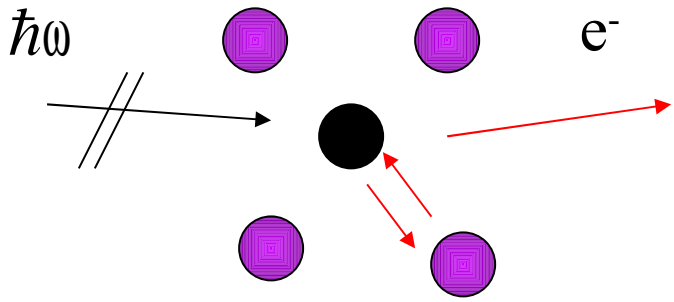

σ_3 – double diffusion – high order correlation functions

$$t_l^0 G\, t_l^i G\, t_{l'}^j G\, t_l^0$$

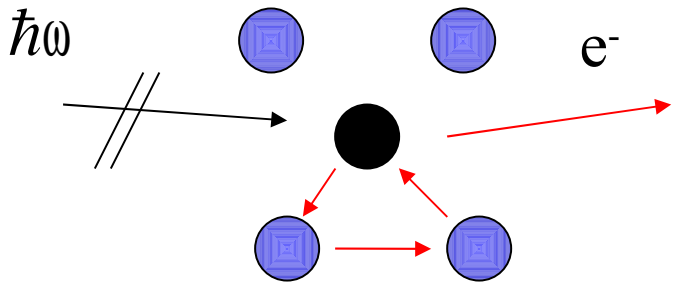

All the structural information are contained in the structural factor

$$\chi^{1}(E) = 1 + \sum_{n=2} \chi^{1}_{n}(E)$$

$$\chi^{1}_{n}(E) = \frac{1}{(2l+1)\sin^{2}\delta^{0}_{l}} \sum_{m} \mathrm{Im}[(T_a G)^{n} T_a]^{00}_{lmlm}$$

partial contribution of order n coming from all process where the photoelectron is scattered n-1 time by the surrounding atoms before escaping to free space after returning to absorbing atom

The interpretation in term of series is valid only if

$$\rho \leq 1$$

In general

$$\rho \underset{k \to \infty}{\longrightarrow} 0 \qquad (t_1 \to 0)$$

$$\rho \underset{k \to 0}{\longrightarrow} \infty \qquad (G \to \infty)$$

$$\begin{cases} \text{High energy} \rightarrow \sigma_0 \text{ or } \sigma_0 + \sigma_2 \\ \text{Low energy} \longrightarrow \sigma_0 + \sigma_2 + \sigma_3 + \ldots. \end{cases}$$

XAS spectrum – three regions

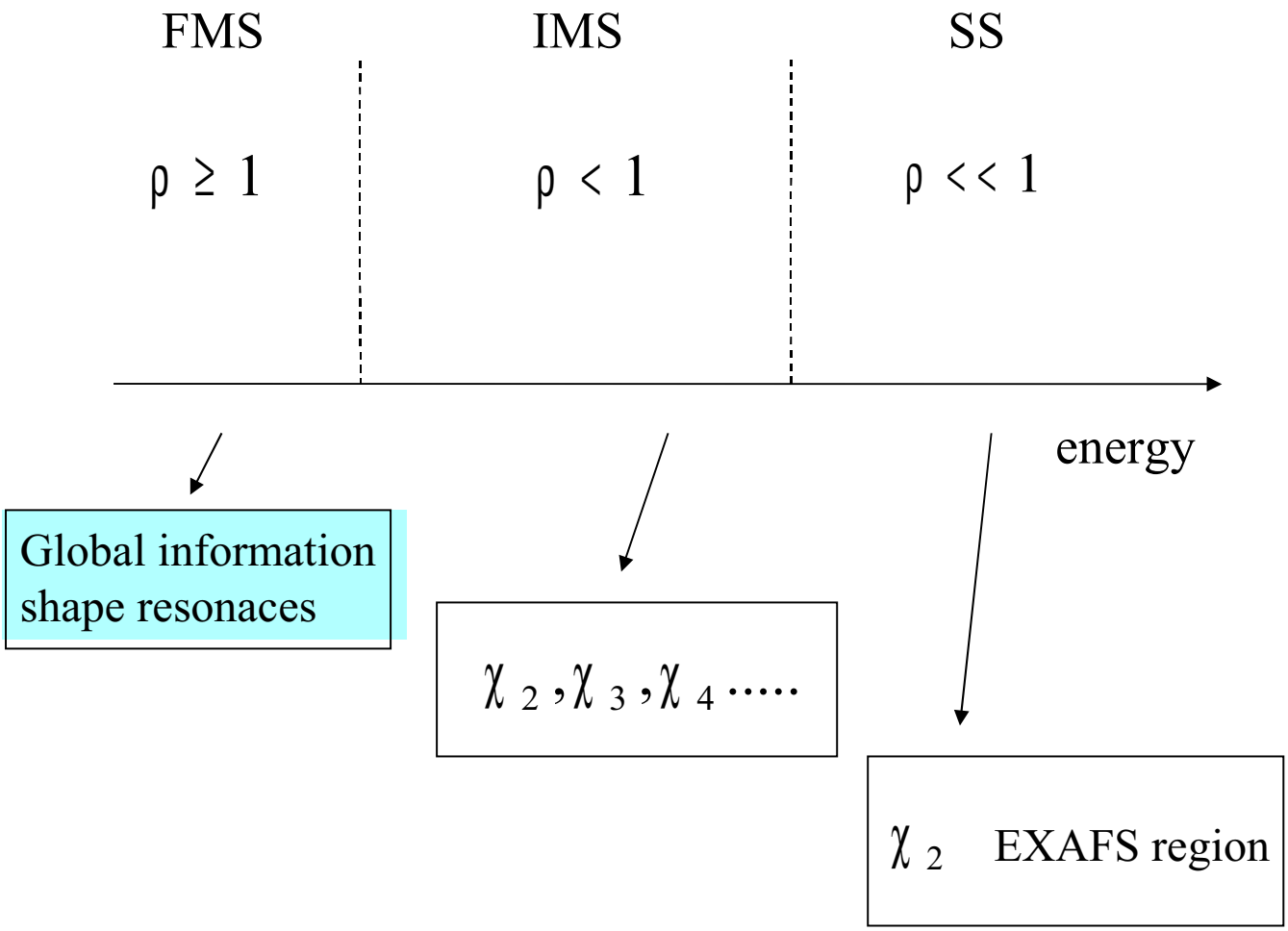

There are cases where $\rho \approx 1$ around 100-150 eV

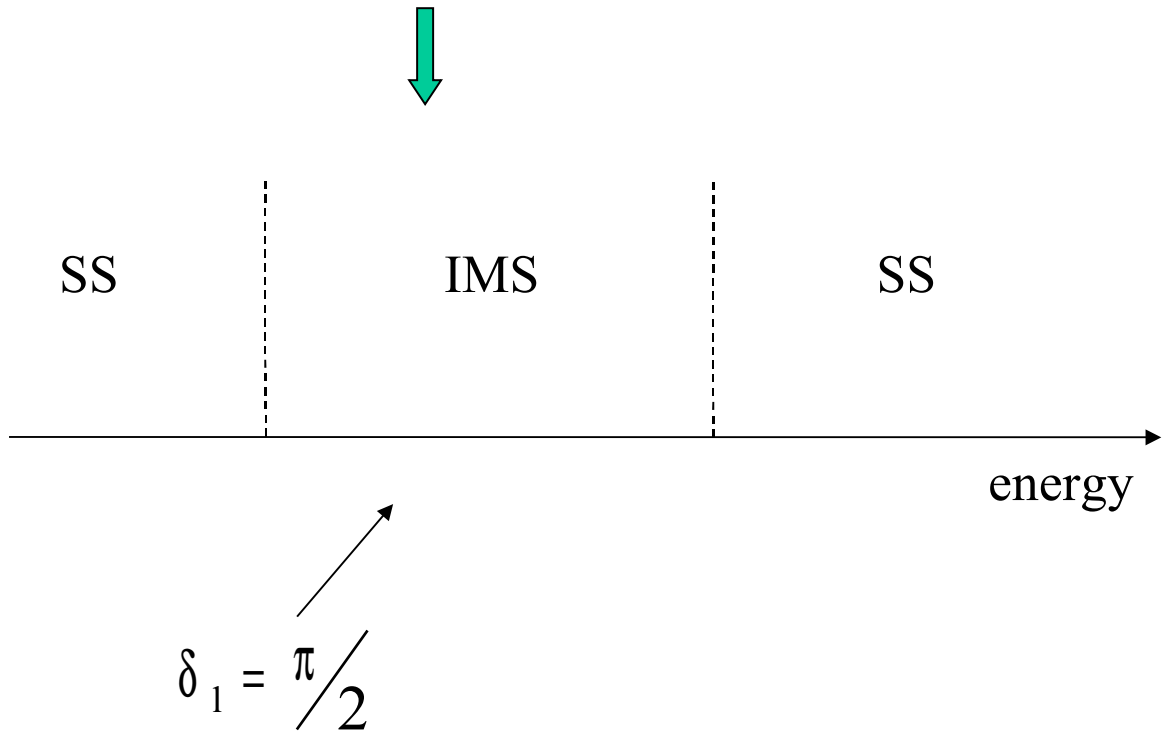

the k-edge of transition metals

Mn K-edge

M. Benfatto et al. PRB **34** (1986)

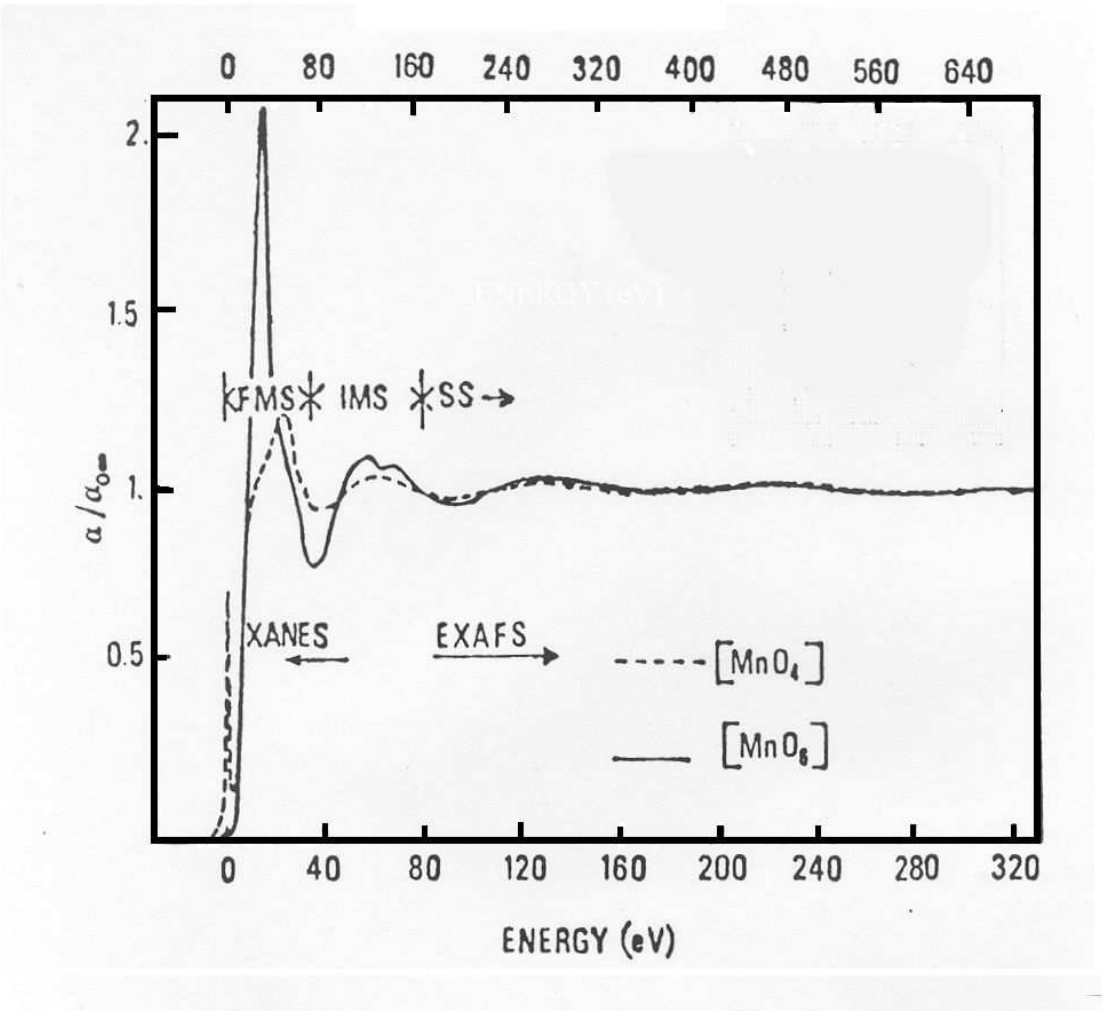

The energy scale are in the ratio 0.47 to account for the different distance between Mn and O in MnO_6 and MnO_4

The amplitude has been corrected for the different number of neighbourings

The two spectra are different below 150 eV → MS contributions

exp

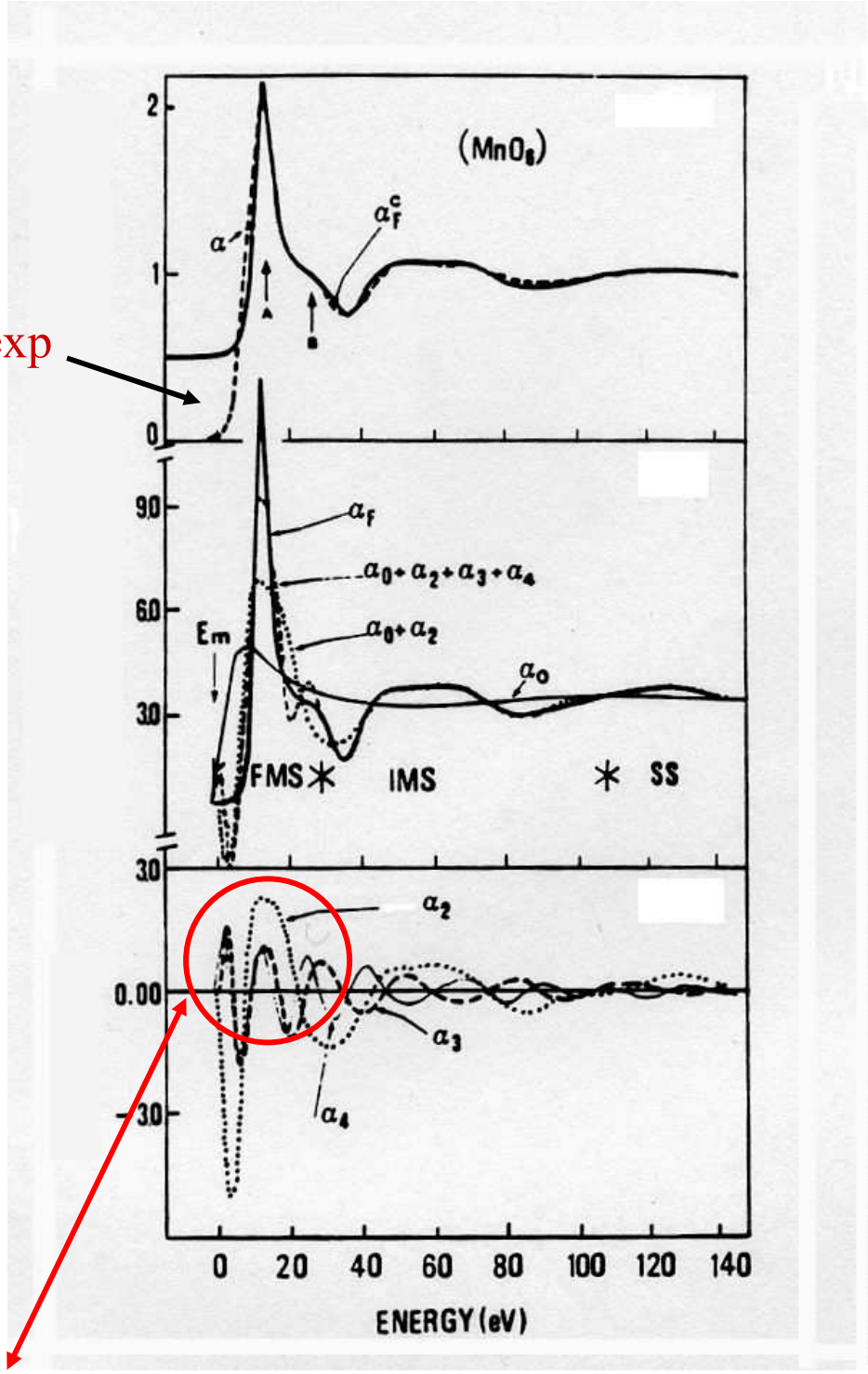

All the MS contributions are at the same energy

Shape resonance

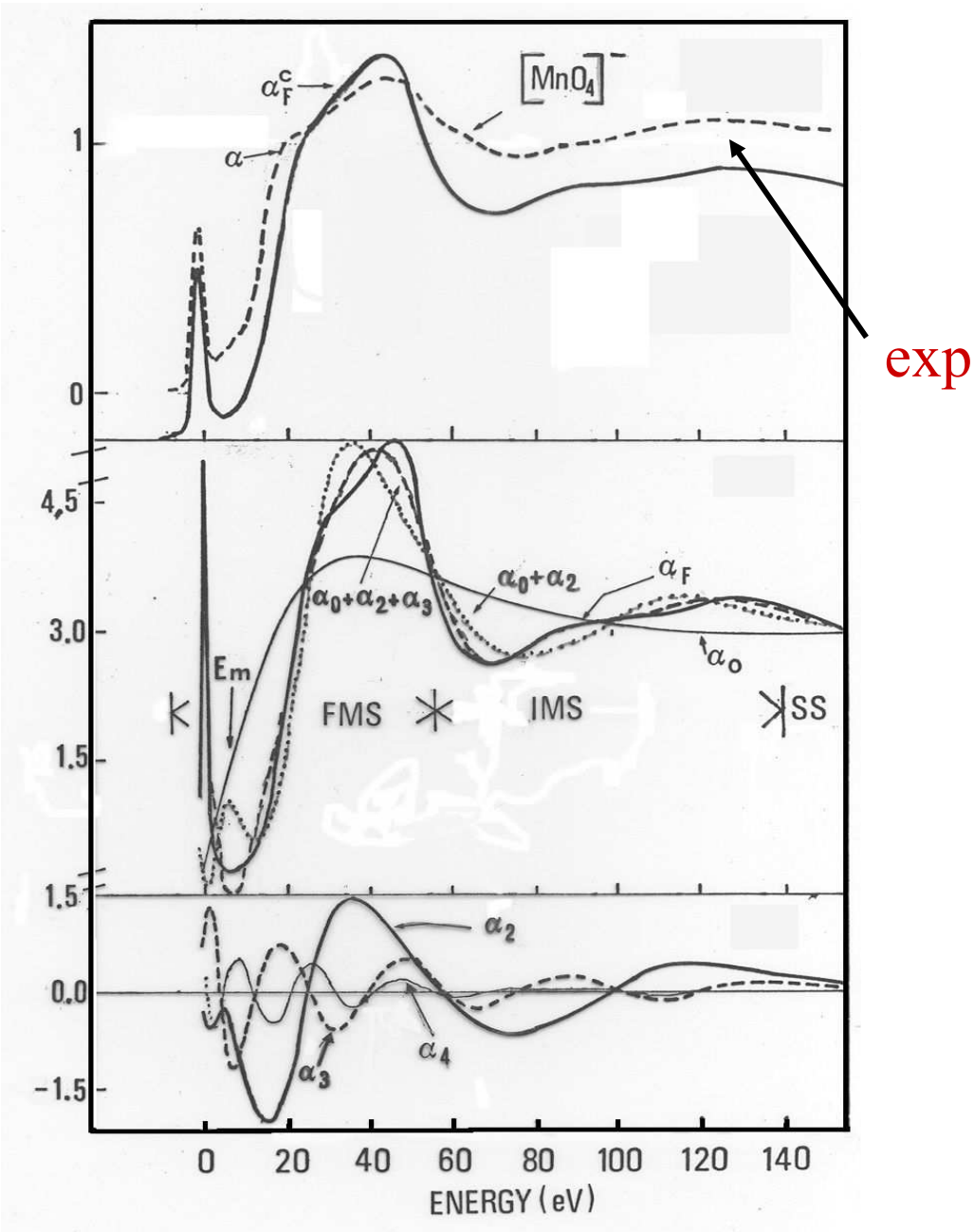

Tetrahedral coordination
Relevant MS contributions up to 150 eV

FMS region

- MS series does not converge $\rho \geq 1$

↓

Many or infinite number of paths contribute to the shape of the spectrum - usually near the edge region (20-40 eV from the edge) for low Z scattering atoms

↓

The scattering path operator must be calculated exactly

Shape resonance → global information

point group symmetry - relations like $k_r R$=const.

Resonance condition

$$\tau = \left[M - i\Delta\right]^{-1} \qquad \mathrm{Det}M(E_r) = 0$$

Mn K-edge in MnO_4

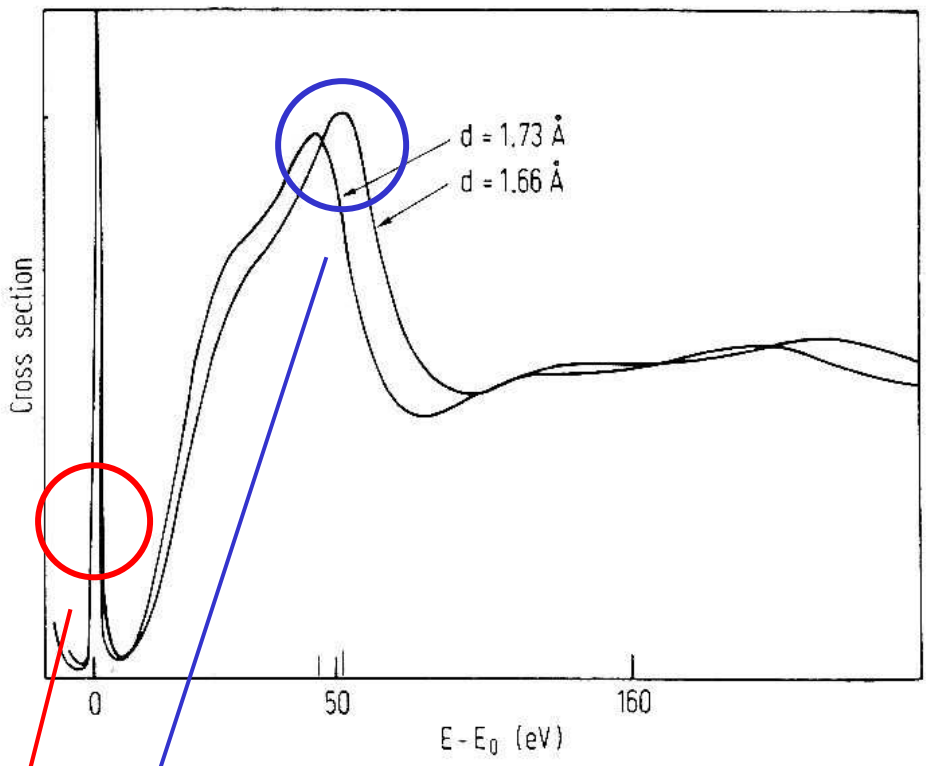

$$|E_b - E_r| R^2 = \text{const} \quad \begin{cases} 139.8 \text{ for } d=1.73 \\ 142.3 \text{ for } d=1.66 \end{cases}$$

IMS and SS regions $\rho < 1$

Typically from 30 eV above the absorption edge

Information on bond lengths and angles

The photoelectron is sensitive to the relative position of two, three or more atoms at the time via the MS paths

Experimental analysis in term of partial contribution $\chi_n^l(E)$

Each term can be written using the (3n-3)-j symbols

Very complicated expressions

but

the functional form

$$\chi_n^l(E) = \sum_{p_n} A_n^l(k, R_{ij}^{p_n}) \sin[kR_{p_n}^{tot} + \varphi_n^l(k, R_{ij}^{p_n})]$$

one can always fit an experimental spectrum with a series of EXAFS like functions.

It is used for making configurational average

Debye-Waller factors

Structural disorder

The calculation of the EXAFS signal

$$\chi_2^l = \frac{1}{2l+1} \sum_{j \neq 0} \sum_{mm'l'} \mathrm{Im}\{e^{2i\delta_l^0} G^{0j}_{lml'm'} t^j_{l'} G^{j0}_{l'm'lm}\}$$

$$\Downarrow$$

$$\chi_2^l = (-1)^l \sum_{j \neq 0} \sum_{l'} \mathrm{Im}\{e^{2i\delta_l^0} (i)^{2l'+1} t^j_{l'} (2l'+1) H(l,l',kR_{j0})\}$$

where

$$H(l,l',kR_{j0}) = \sum_{l''} (i)^{l''} (2l''+1) \begin{pmatrix} l & l' & l'' \\ 0 & 0 & 0 \end{pmatrix}^2 (h^+_{l''}(kR_{j0}))^2$$

All other signals can be derived in the same way by 3j, 6j, 9j symbols.

Plane wave approximation

$$(i)^l \, h_l^+ \, (kR) \rightarrow \frac{e^{ikR}}{kR}$$

$$\chi_2^l = (-1)^l \sum_{j \neq 0} \mathrm{Im}\{e^{2i\delta_l^0} \frac{e^{2ikR_{j0}}}{kR_{j0}} F_j(k)\}$$

$$F_j(k) = \frac{1}{k} \sum_l (i)^{2l+1} (2l+1) e^{i\delta_l^j} \sin\delta_l^j$$

The phase does not depend by the distance

some conclusions

- Core levels are spatially localized
- Every atom has a well defined core levels

⇓

site selectivity

The photoelectron probes the system

↓

Strong interaction with the matter

⇓

Infomation beyond the pair correlation functions

We need to account for other physical processes

- inelastic excitations suffered by the photoelectron
- electronic excitations due to the creation on core-hole
- finite core hole width
- …….

They drain away amplitude from the elastic channel and must be included in any realistic calculation

↓

finite lifetime of the photoelectron in the final state

↓

many-body treatment of the photoabsorption process

$$\sigma(\omega) = 4\pi^2\alpha\,\omega \sum_f \left|\left\langle \Psi_f^N \middle| \vec{\varepsilon}\cdot\vec{r} \middle| \Psi_G^N \right\rangle\right|^2 \delta(\omega - E_f + E_c)$$

Many body final and ground state w.f.

$$\Psi_G^N(\vec{r}, \vec{r}_1 \ldots \vec{r}_{N-1}) = \sqrt{N!}\, A\, \phi_{L_0}^c(\vec{r})\, \Psi_G^{N-1}(\vec{r}_1 \ldots \vec{r}_{N-1})$$

antisymmetrization operator core level

$$\Psi_G^{N-1}(\vec{r}_1 \ldots \vec{r}_{N-1}) = \sum_n C_n \phi_n^{N-1}(\vec{r}_1 \ldots \vec{r}_{N-1})$$

Slater determinants

for the final state

$$\Psi_f^N(\vec{r},\vec{r}_1\ldots\vec{r}_{N-1}) = \sqrt{N!}\,A\sum_\alpha \phi_\alpha^f(\vec{r})\Psi_\alpha^{N-1}(\vec{r}_1\ldots\vec{r}_{N-1})$$

excited photoelectron

final state channels w.f. relaxed around the core hole

$$H_{N-1}\Psi_\alpha^{N-1} = E_\alpha^{N-1}\Psi_\alpha^{N-1}$$

$$(\nabla^2 + k_\alpha^2)\phi_\alpha^f(\vec{r}) = \sum_\beta \int V_{\alpha\beta}(\vec{r},\vec{r}\,')\phi_\beta^f(\vec{r}\,')\,d\vec{r}\,'$$

where

$$k_\alpha^2 = \omega - I_c - \Delta E_\alpha$$

Interchannels potential depending also to non-local exchange term

ionization potential

excitation energy left behind in the (N-1) particle system

It is convenient to introduce the Green functions writing the total photoabsorption cross section

$$\sigma(\omega) \propto \sum_{m_0,\sigma_0} \int d^3r d^3r' \phi^c_{L_0}(\vec{r})\vec{\varepsilon}\cdot\vec{r}\,\mathrm{Im}\left\{\sum_{\alpha,\alpha'} S^*_\alpha S_{\alpha'} G_{\alpha,\alpha'}(\vec{r},\vec{r}';\omega - I_c)\right\}\vec{\varepsilon}\cdot\vec{r}'\phi^c_{L_0}(\vec{r}')$$

$$S_\alpha = \left\langle \Psi^{N-1}_\alpha \middle| \Psi^{N-1}_G \right\rangle$$

$$G_{\alpha,\alpha'}(\vec{r},\vec{r}';E) = \sum_f \frac{\phi^f_\alpha(\vec{r})\phi^f_{\alpha'}(\vec{r}')}{E - \Delta E_f - i\eta}$$

$$\Delta E_f = E_f - E_G$$

$$E_f = E_G + \omega$$

The Green's-functions matrix satisfies a set of coupled equations that contains the complete description of all the possible outcomes of a photoemission process

Two possibilities

the complete relaxed channel dominates $\Delta E_\alpha = 0$

Different channels

$$\sigma(\omega) \propto \mathrm{Im}\left|S_0(\omega)\right|^2 G_{00}(\omega - I_c)$$

$$\sigma(\omega) \propto \mathrm{Im}\sum_{\alpha,\alpha'} M_L^{\alpha}\, \tau^{\alpha,\alpha'}_{0L,0L}\, M_L^{\alpha'}$$

$$\tau = S^{-1}$$

$$S = \begin{matrix} [\tau_o^{-1}]^{\alpha_0} & [K^{-1}]^{\alpha_0\alpha_1} & .. \\ [K^{-1}]^{\alpha_1\alpha_0} & [\tau_o^{-1}]^{\alpha_1} & .. \\ .. & .. & .. \end{matrix}$$

τ_o is the usual scattering path operator for the channel α with the k_α wave-vector

If only one electronic configuration dominates, typically the complete relaxed channel $\Delta E_\alpha = 0$

We can eliminate from the set all channels which give rise to similar interchannels potential

Plasmon type – delocalized in the system

$$\sigma(\omega) \propto \mathrm{Im}\left|S_0(\omega)\right|^2 G_{00}(\omega - I_c)$$

it satisfies a Dyson equation with optical potential

$$\left[\nabla^2 + E - V_c(\vec{r}) - \Sigma_{exc}(\vec{r};E)\right] G^+_{00}(\vec{r},\vec{r}';E) = \delta(\vec{r} - \vec{r}')$$

$$\Sigma_{exc}(\vec{r};E) = V(\vec{r};E) + i\Gamma(\vec{r};E)$$

from many body to on effective one particle problem

Some considerations

- in metal one obtains very good agreement with the experimental data using a one-particle approach with an X-α potential and convoluting the calculated spectrum with a Lorentzian broadening function having an energy-dependent width.

- double-electron excitations are normally very weak, typically 10^{-2} – 10^{-3} times the main relaxed channel

we choose the Hedin-Lundqvist (HL) potential extending its validity in to the atomic core region

it has an imaginary part that is able to reproduce the observed mean-free path in metal. This part starts at the plasmon energy

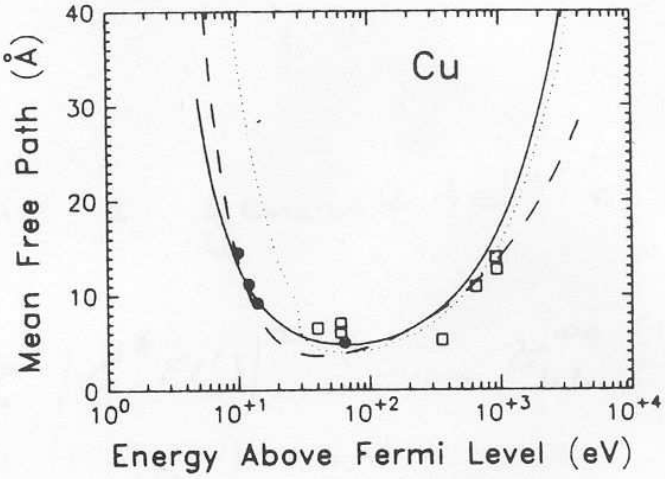

FIG. 1. Inelastic electron mean free path versus energy above the Fermi energy for Cu. Solid curve is present theory. Dotted curve is theory of Tung *et al.* (Ref. 1). Dashed curve is from Seah and Dench (Ref. 8). Experimental data: solid circles, Refs. 10 and 11; open squares, Ref. 14.

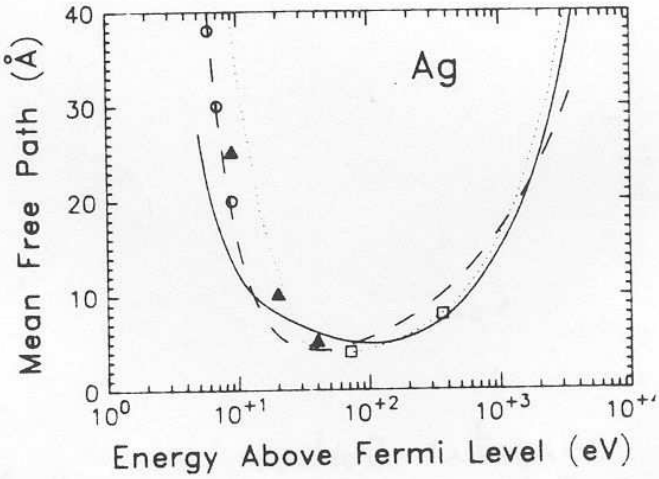

FIG. 2. Same as Fig. 1 but for Ag. Experimental data: open circles, Ref. 15; solid triangles, Ref. 16; open squares, Ref. 17.

Inelastic electron mean free path

For a muffin-tin type of potential

$$G^{+}_{00}(\vec{r},\vec{r}';E) = -k\sum_{L,L'} R^{0}_{L}(\vec{r})\,\tau^{00}_{LL'}\,R^{0}_{L'}(\vec{r}') + \sum_{L} R^{0}_{L}(\vec{r})S^{0}_{L}(\vec{r}')$$

usual scattering path operator

total structural signal in a final angular momentum channel l

$$\chi_{l}(E) = \frac{\sigma_{l}(E)}{[\sigma_{a}(E)]_{l}} - 1$$

MS signals of order n

$$\chi^{n}_{l}(E) = \frac{\sigma^{n}_{l}(E)}{[\sigma_{a}(E)]_{l}}$$

The use of complex potential automatically introduces a damping in the the elastic signal

$$G_{LL'}^{ij} \approx \frac{e^{ikR_{ij}}}{kR_{ij}}$$

If $k = k_r + i\, k_i$ we have a decreasing exponential

$$\lambda_{tot} = \frac{1}{k}\frac{E}{\Gamma_{tot}(E)}$$

The presence of several possible electronic excitations beyond the elastic one “creates” the concept of the electronic inelastic mean free path

we see only few shells around the absorber typically 5-10 at the edge

To account for that we have introduced an optical potential with a complex part – Within some conditions this is completely equivalent to a convolution of the real calculation

S K-edge in ZnS

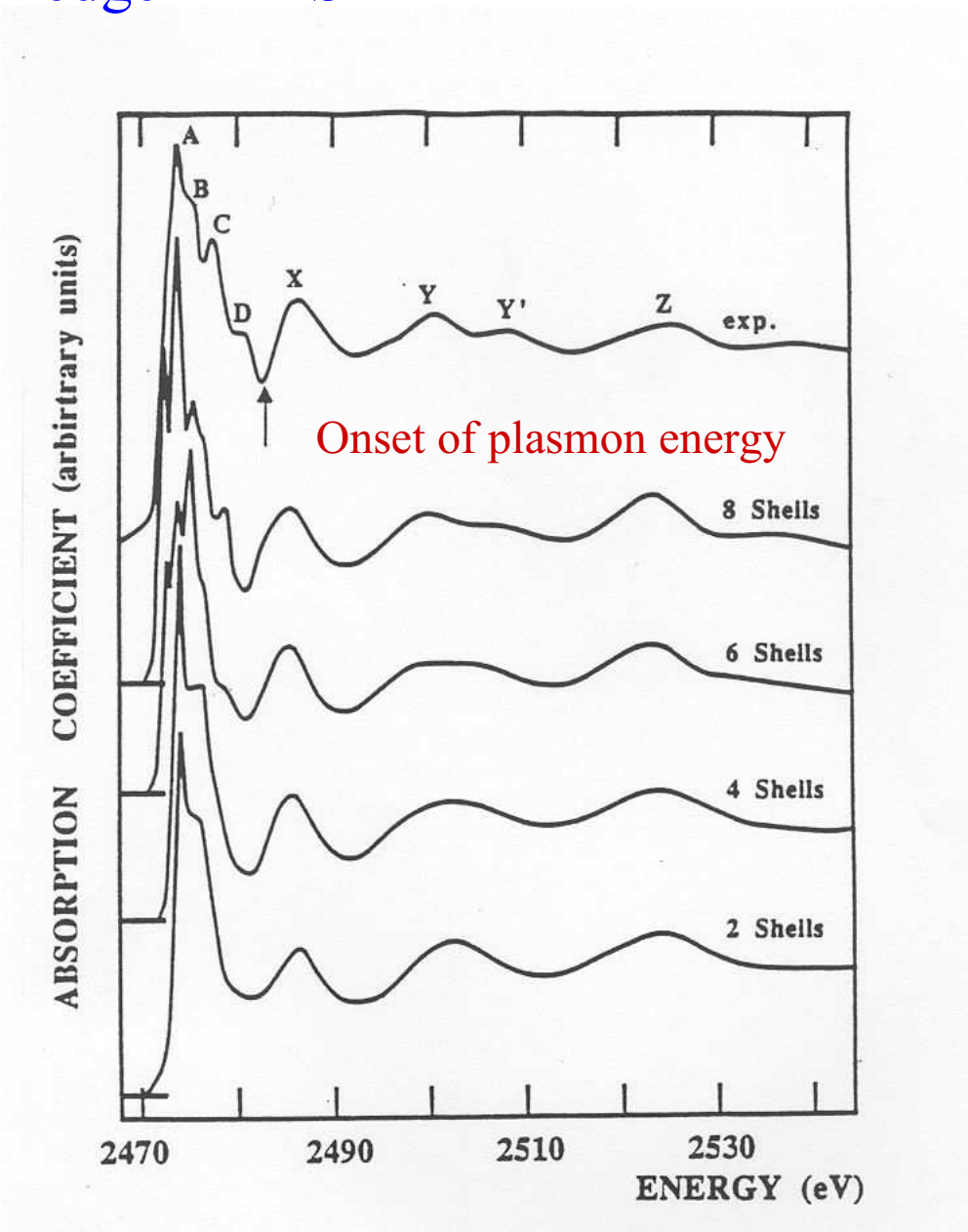

The cross section has been built shell by shell

Si K-edge crystal silicon

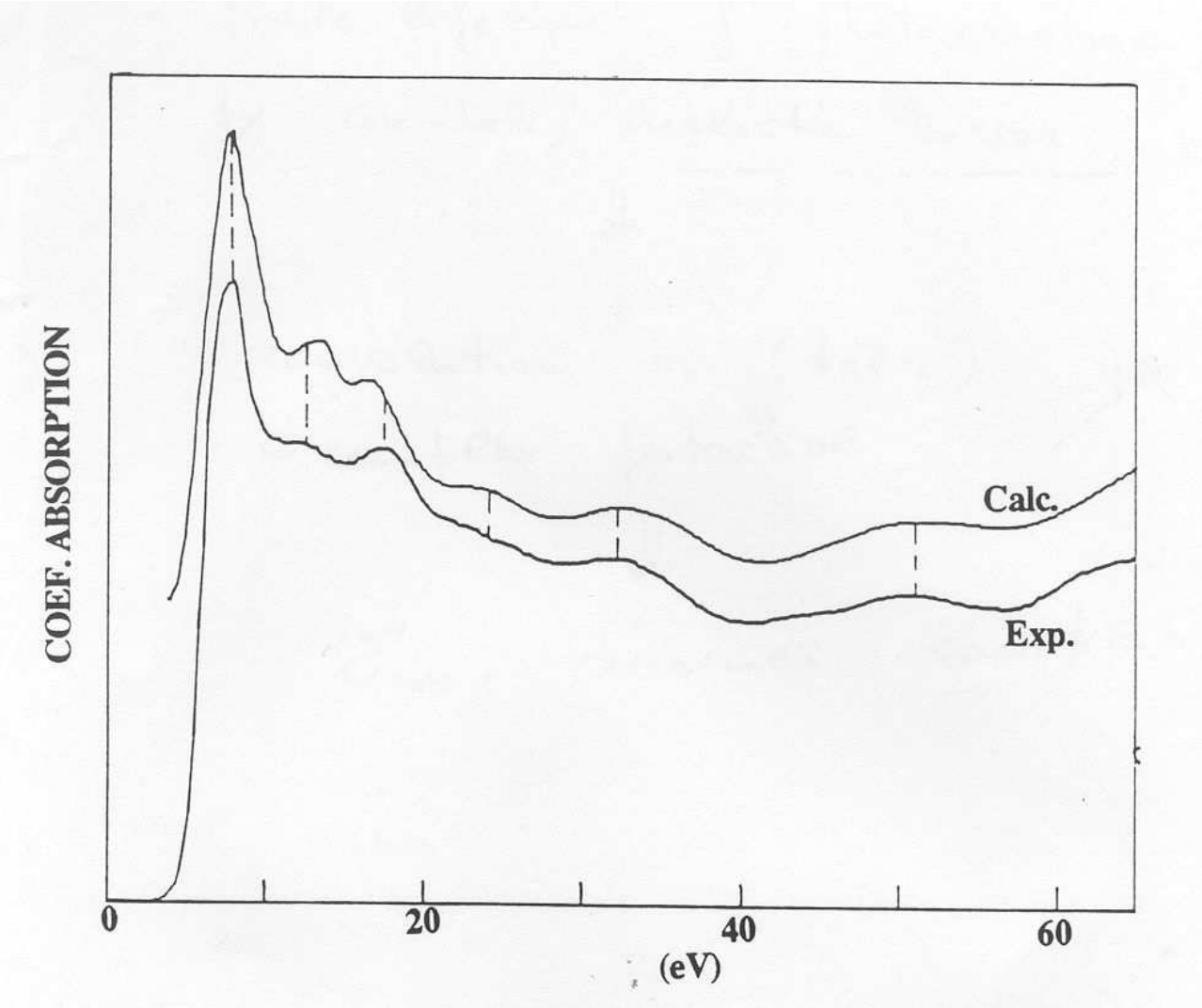

8 shells around the absorber

The case of several electronic configurations

Several systems can generate K-edge XANES with "extra" peaks due to the presence of different electronic configurations

Some cuprates – the Cu K-edge – $3d^9 + 3d^{10}\underline{L}$

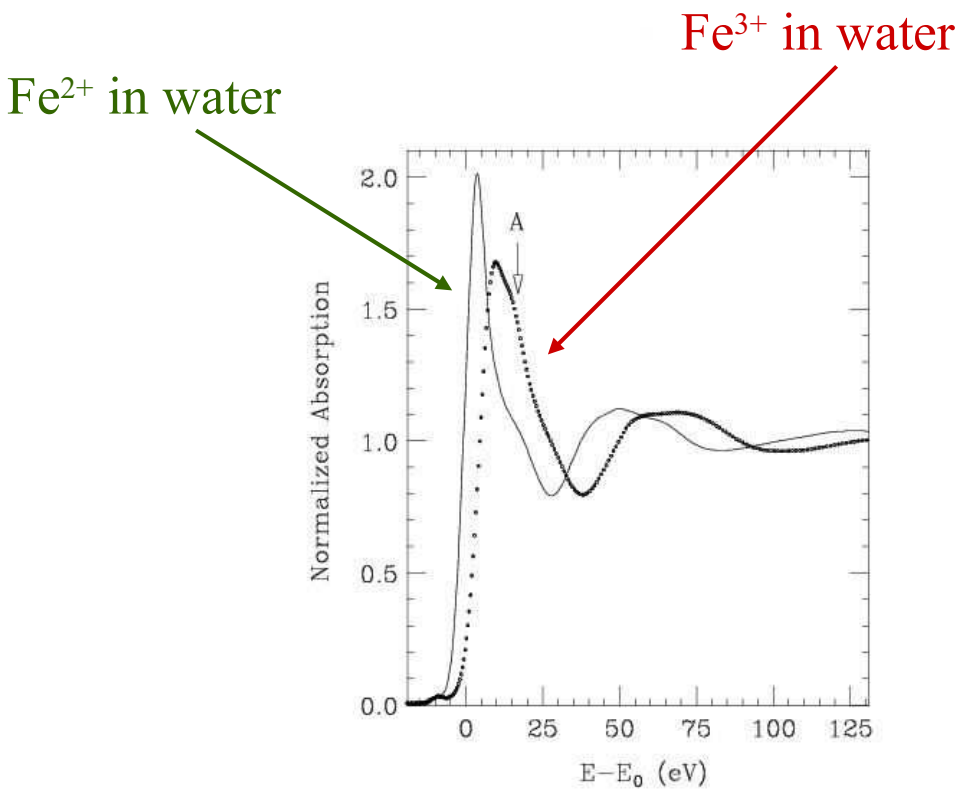

$$K^{-1} \xrightarrow[E \to \infty]{} 0$$

reactance matrix

The different channels decouple at high energy

$$\sigma(\omega) = a^2 \sigma_0(k_0) + b^2 \sigma_1(k_1) + \ldots$$

$$k_0^2 = \hbar\omega - I_c$$

$$k_1^2 = \hbar\omega - I_c - \Delta E_1$$

.....

The total cross section is the sum of independent spectra shifted in energy

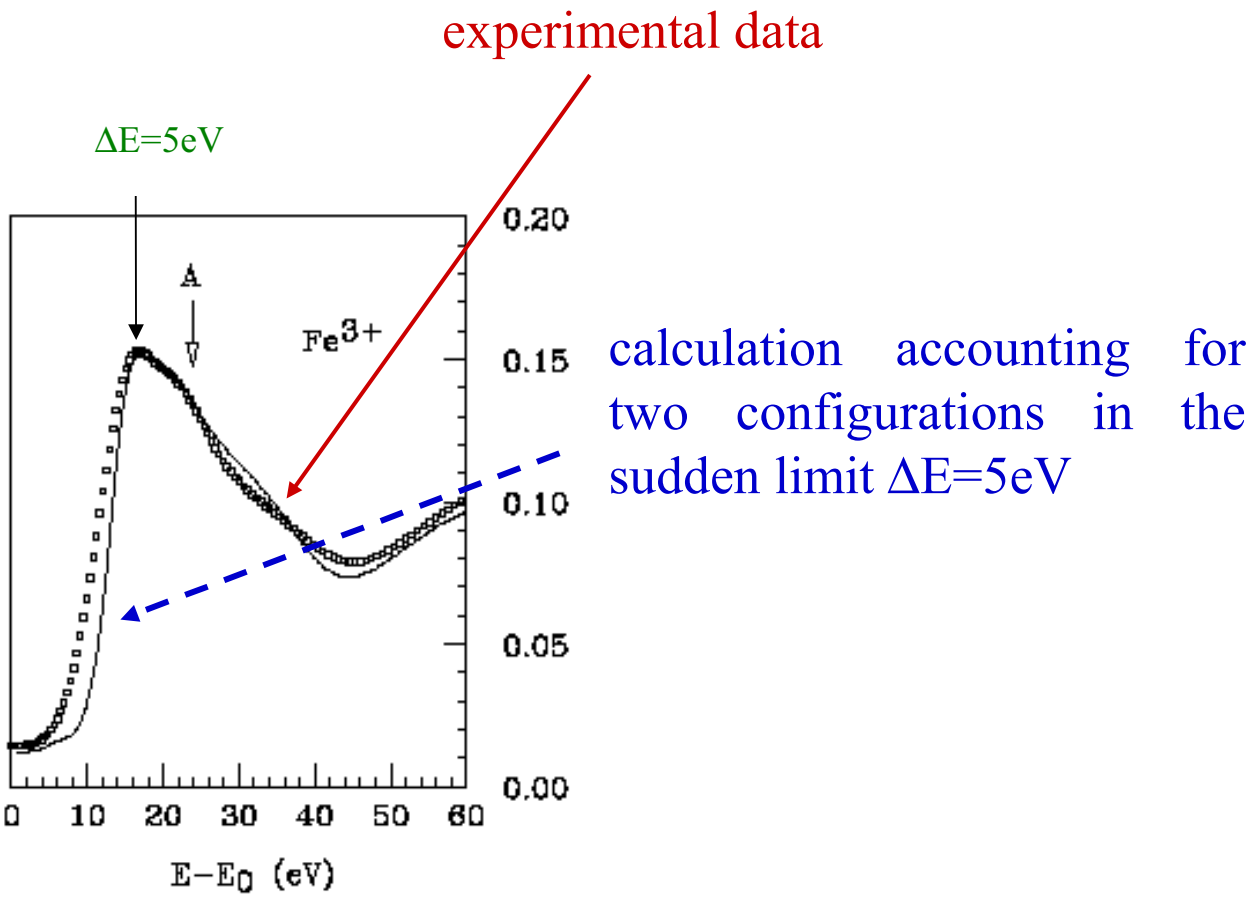

The extra feature A is explained by the presence a second electronic configuration generated by moving one electron from low- to high-t_{2g} level. SCF calculation gives an energy separation ΔE=5 eV

but

Problems for a quantitative structural determination

How to get structural information

Methods essentially based on FT and the concept of phase transferability, normally they are limited to the first shell analysis and systems with negligible MS contribution

These methods use mainly the EXAFS part of the spectrum

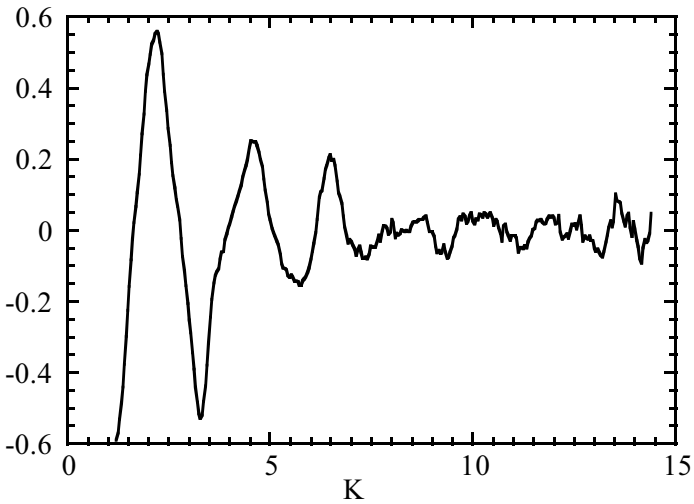

→ F.T.

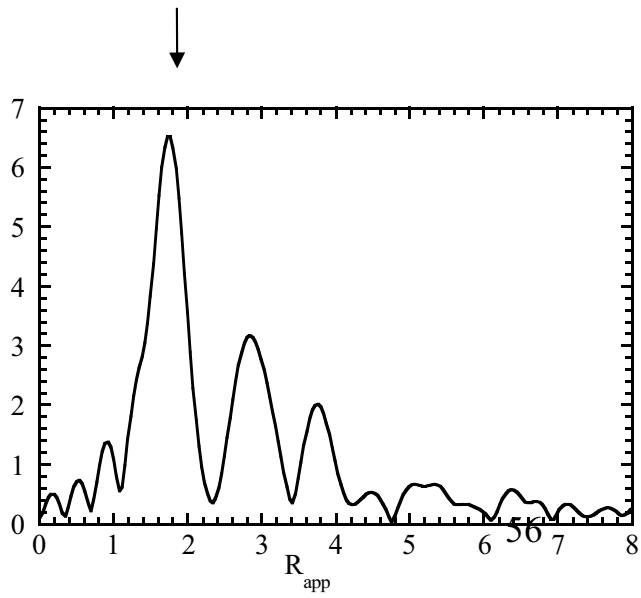

Other methods are based on fit procedure that use the MS approach to generate the theoretical MS series, i.e. χ_n many signals to be compared with exp. data. By moving bond lengths and angles those programs reach the best fit conditions in term of structural used parameters.

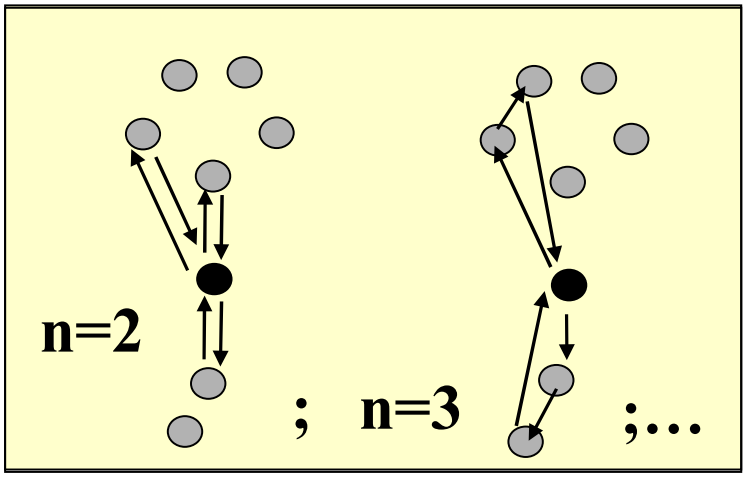

Feff --- EXCURVE

Normally the XANES energy region is used on the basis of qualitative manner

Recently we have developed a new method to use XANES (from edge to about 200 eV) as a source of **quantitative** structural information.

⟵ Why?

Many XAS spectra "contain" most of the structural information in XANES energy region, in particular biological samples because the scattering power decreases very rapidly with the energy in light elements.

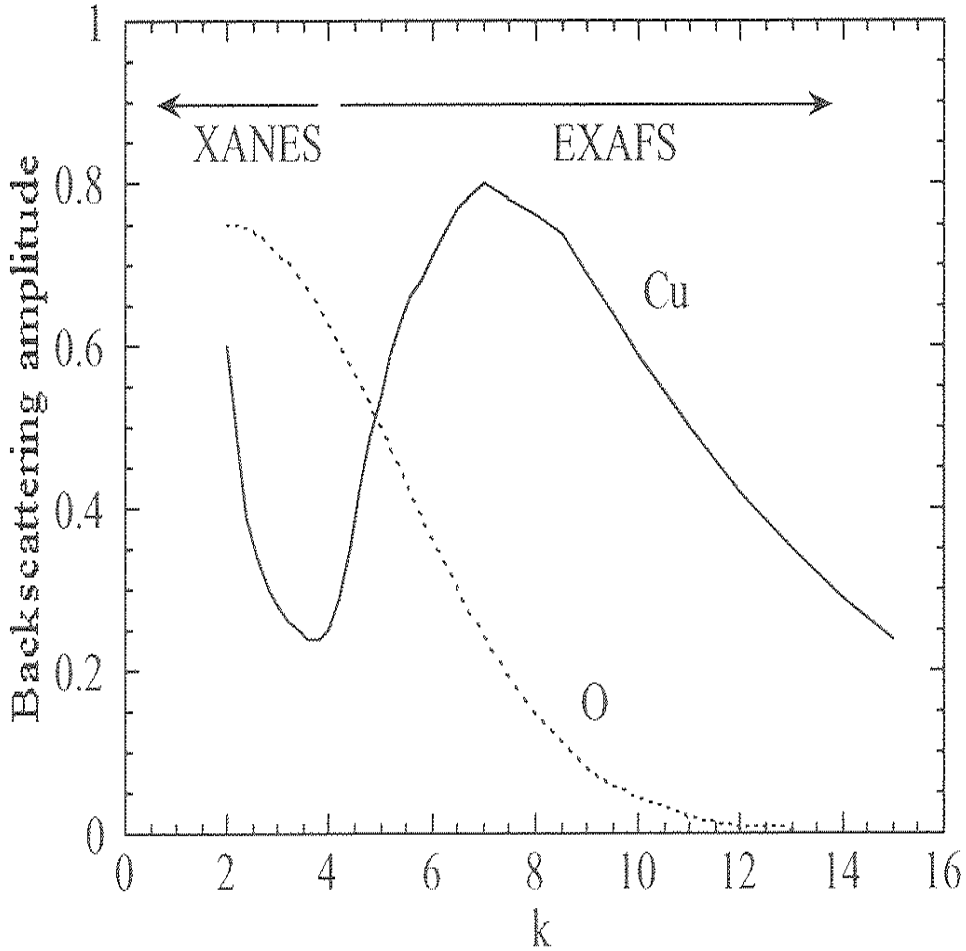

$$F_j(k) = \frac{1}{k}\sum_l (i)^{2l+1}(2l+1)e^{i\delta_l^j}\sin\delta_l^j$$

Biological example

Low temperature photolysis of myoglobin

$$\text{MbCO} \xrightarrow[T < 40K]{h\nu} \text{Mb*CO}$$

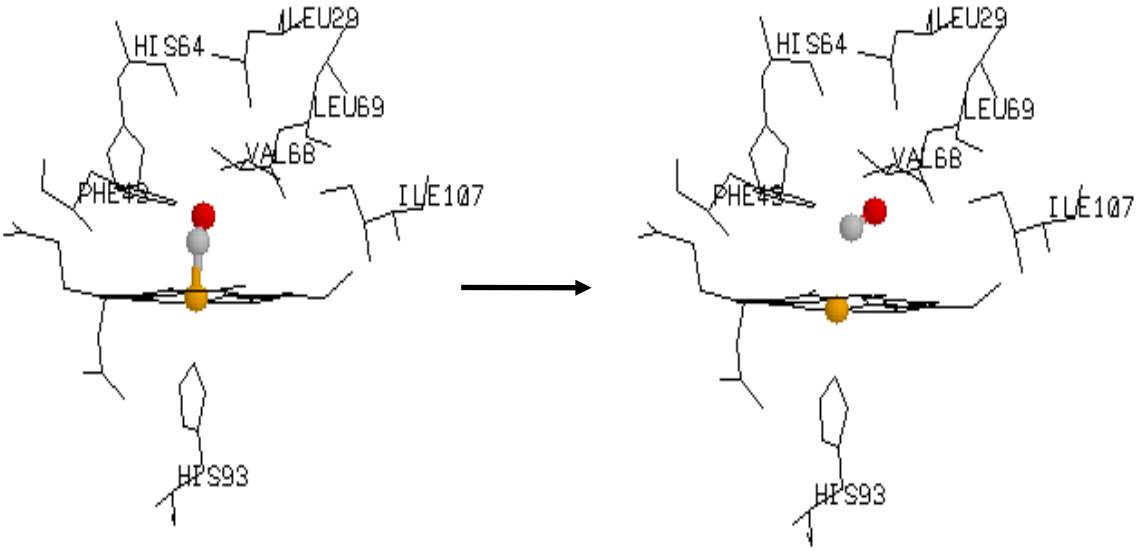

Exp. by S. Della Longa et al. J. Synch. Rad. (1999) **8**, 1138

myoglobin single crystal

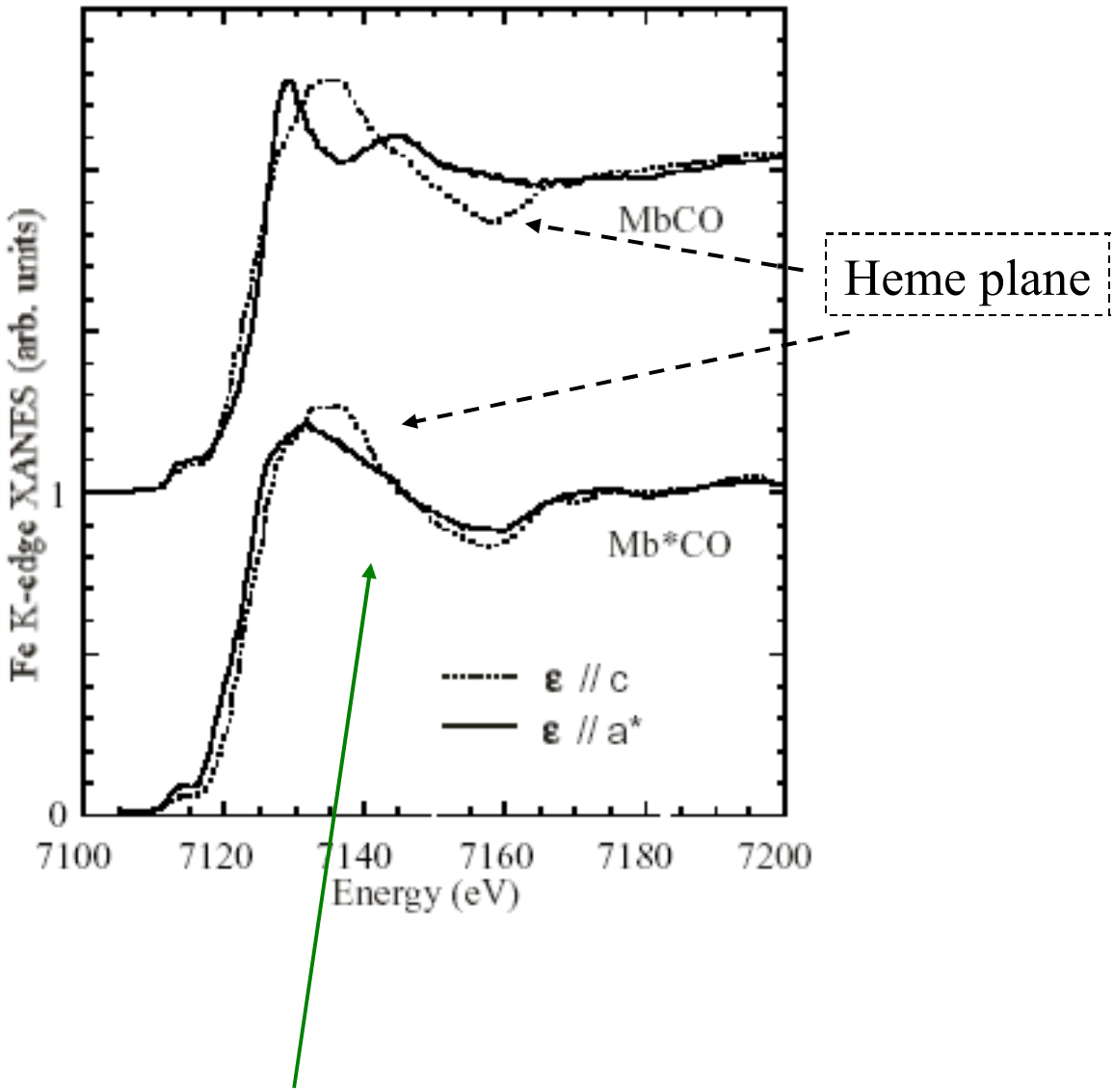

Most of the differences are in the energy range 0 – 80 eV

Two ways to calculate the scattering path operator

- by series:
- Exactly: all MS contributions are included

We have developed a new fitting method, called MXAN, that use the <u>exact calculation</u> of the scattering path operator

i) We work in the energy space
ii) We can start from the edge
iii) We can use polarization dependent spectra

The MXAN method

- Initial geometrical configurations
- Exp. data

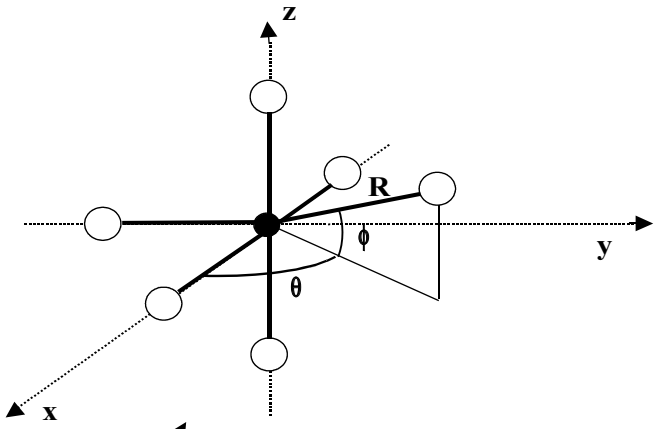

We generate hundred of theor. spectra by moving atomic coordinates

The potential is calculated at each step – Norman criterion

Minimization of error function

$$R_{sq}^{2} = \sum_{i=1}^{N} \{[y_i^{th.}(..r_n, \theta_n, ..) - y_i^{exp.}]^2 / \varepsilon_i^2\} w_i / \sum_{i=1}^{N} w_i$$

By comparison with exp. data we can fit relevant structural parameters

M. Benfatto M and S. Della Longa, Journ. Synch. Rad. (2001), **8** 1087

EXCHANGE and CORRELATION PART

- Complex HL potential + Lorentzian function with a constant Γ_c to account for the core-hole and the experimental resolution

Problems in molecular cluster at low energy, typically in the range 0-30 eV.

Test

Ni^{2+} in water – K-edge of Ni

The calculation at the best fit condition include the H atoms

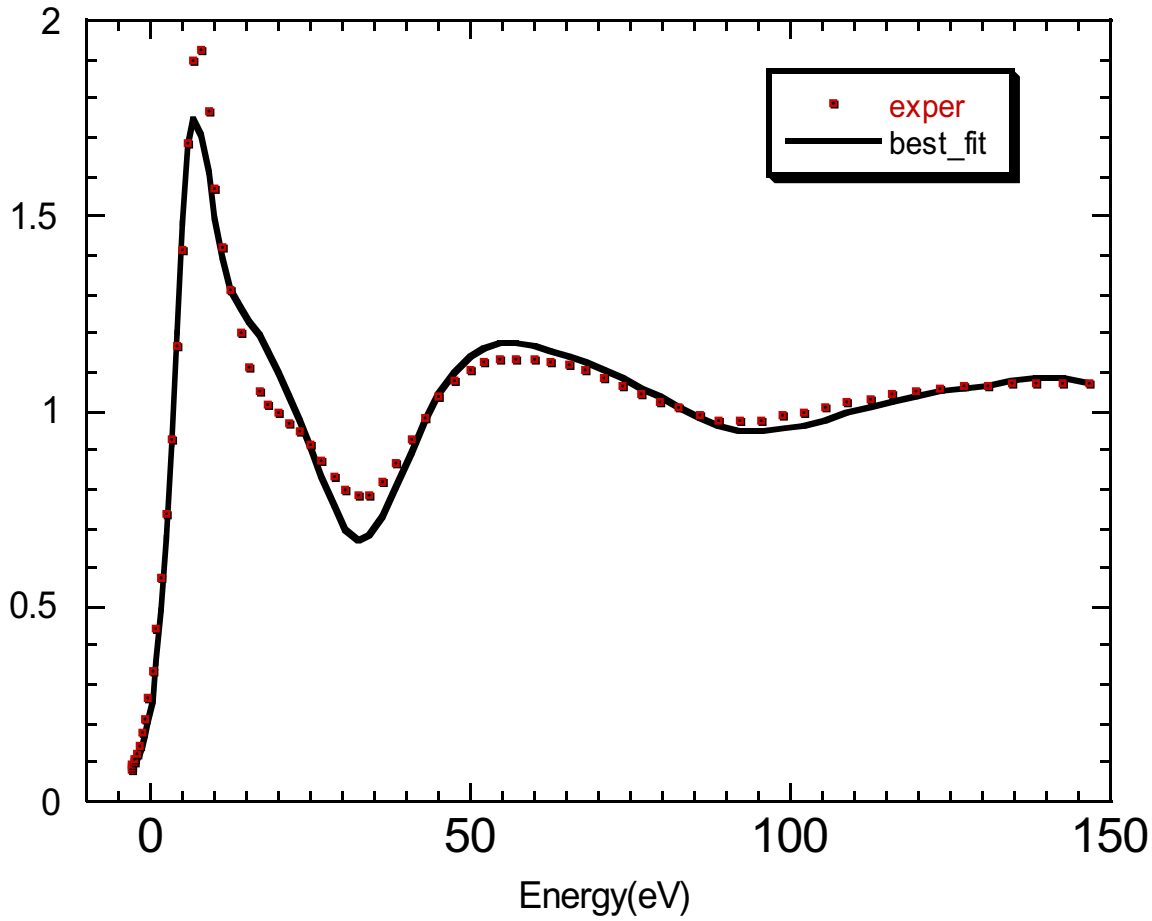

It corresponds to an octahedron with a Ni-O distance of 2.04 Å

The GNXAS and FEFF analysis gives about 2.07 Å

Real HL potential + convolution via a Lorentzian function with $\Gamma_{tot}(E)=\Gamma_c+\Gamma(E)$

$\Gamma(E)$ Behaves like the universal form (Muller et. al., Sol. State Comm. 1982) and starts from energy E_s with a jump A_s. Both E_s, Γ_c and A_s are derived at each step of computation on the basis of Monte Carlo fit.

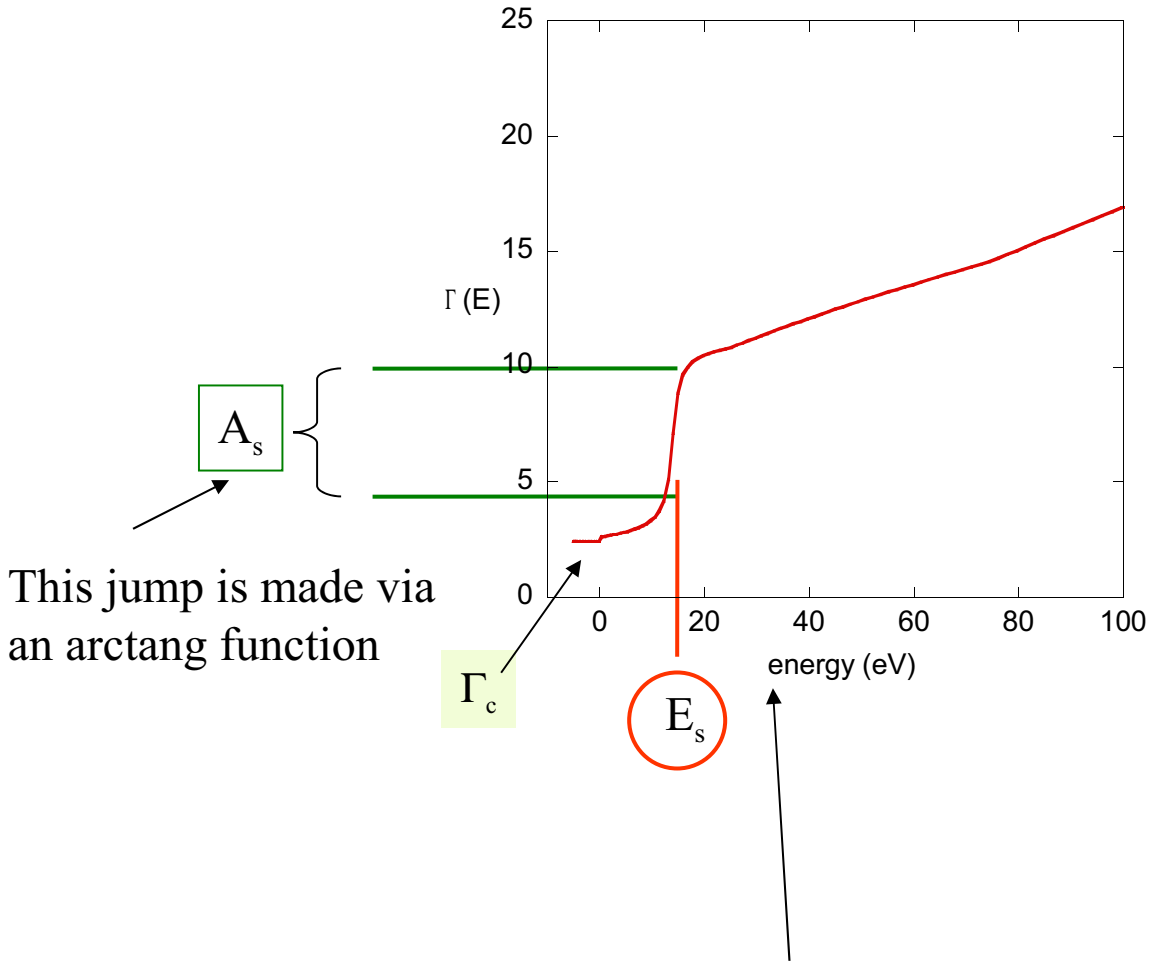

$\Gamma(E)$ contains all the intrinsic and extrinsic inelastic processes

Transition metals in water solution

-Starting condition: distorted orthorhombic symm.
-The fits include Hydrogen atoms

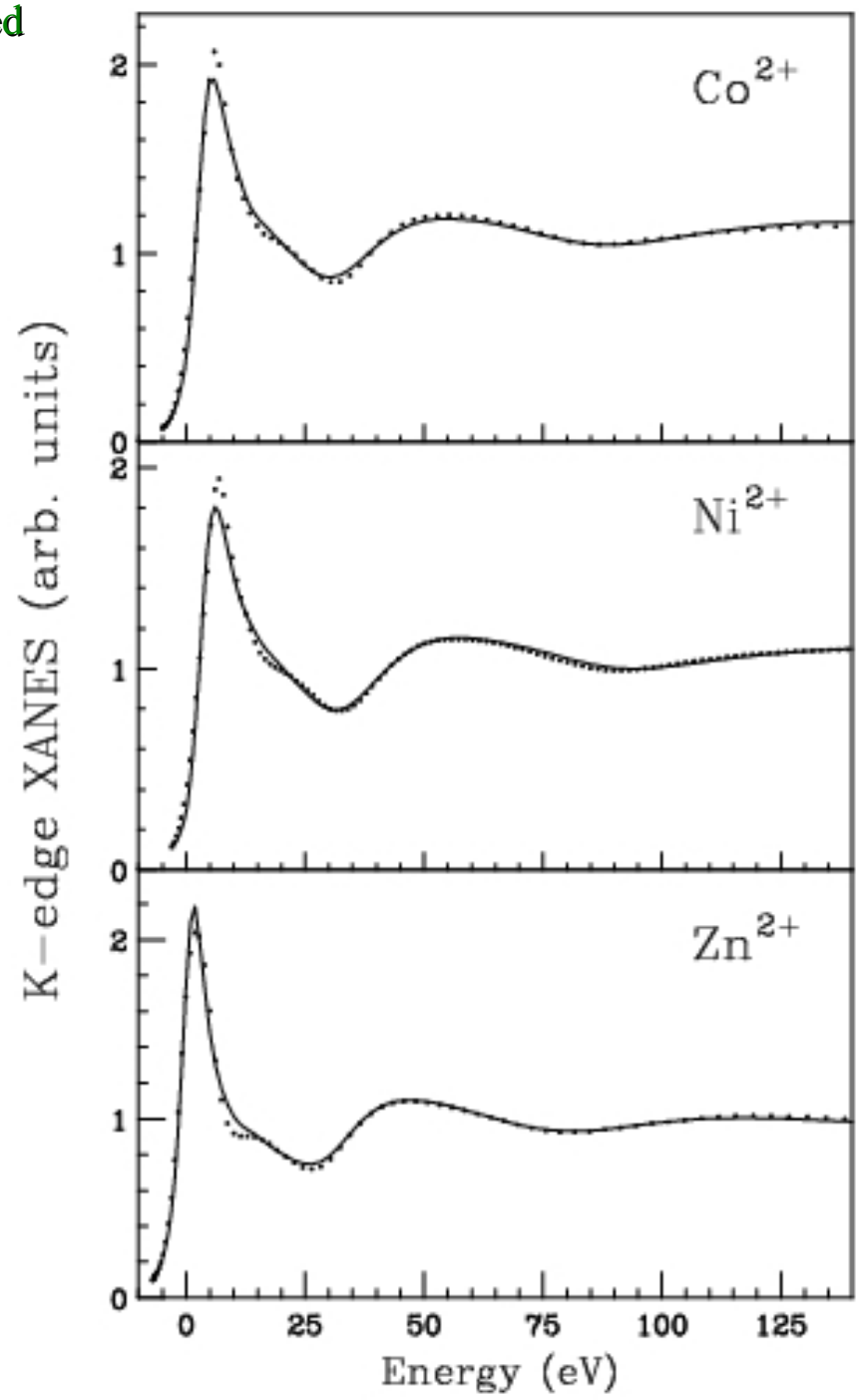

Best fit conditions

Octahedral symmetry

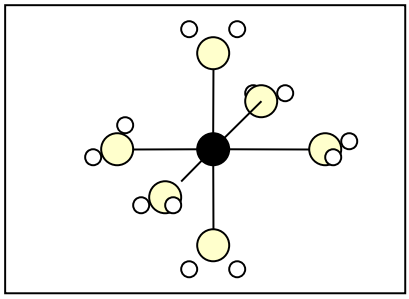

	R(Å)	R(Å)	Γ_c	Γ_{c-h}
Co^{2+}	2.06(0.03)	2.092(0.002)	2.07	1.33
Ni^{2+}	2.03(0.03)	2.072(0.002)	1.70	1.44
Zn^{2+}	2.06(0.02)	2.078(0.002)	3.14	1.67

MXAN

GNXAS

$Fe(CN)_6$ in water

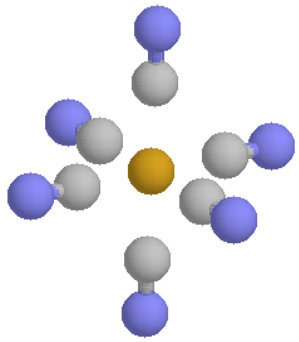

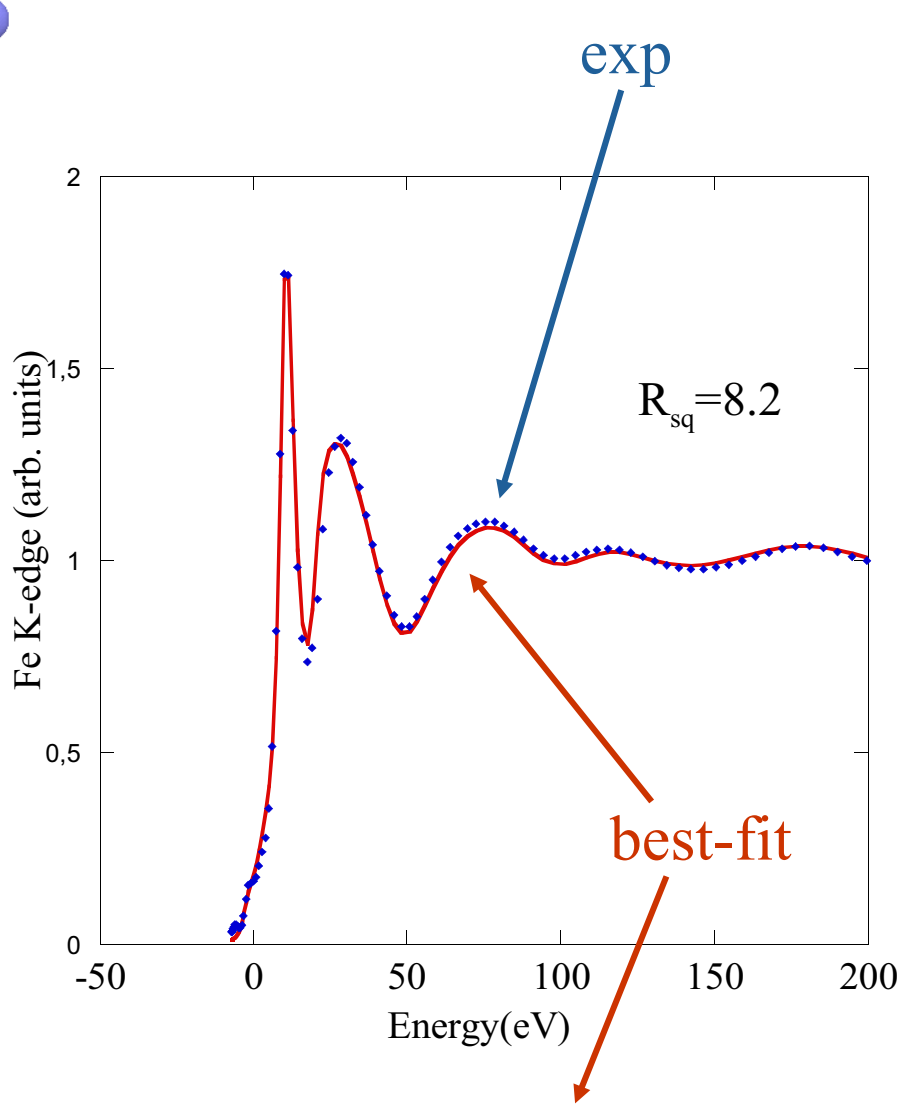

The best-fit condition corresponds to an octahedral symmetry with Fe-C distance of 1.92(0.01) Å and C-N distance of 1.21(0.01) Å

Previous GNXAS analysis (Westre et al. JACS 117 (1995)) reports Fe-C and Fe-N distances of 1.92 Å and 1.18 Å respectively

Fit with NO molecules
Fe-N =1.91Å and N-O =1.16Å

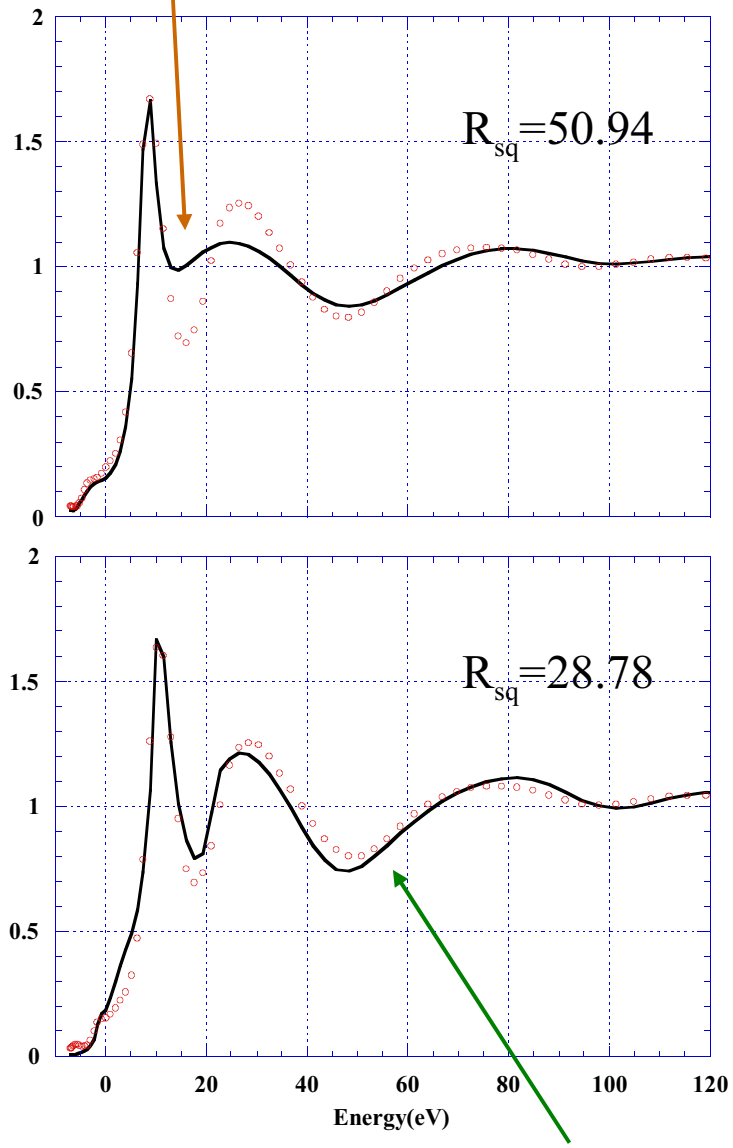

Fit with CO molecules
Fe-C =1.94Å and C-O =1.11Å

Chemical sensitivity

Test cases indicate a good structural reconstruction at the atomic resolution

high sensitivity to the structural changes

the fit results are weakly affected by the errors in the potential determination

↓

just an increase of the error bar in the structural numbers

Three key points:

The use of a phenomenological damping

The potential is calculated at each step of the atomic movement keeping the same Norman criterion

The used energy range is wide enough to minimize errors in the potential determination

Coordination geometry of Cu^{2+} in solution

- Fivefold or sixfold coordination?

- J.T. distortion?

Car – Parrinello molecular dynamics calculation
A. Pasquarello et al. Science (2001)

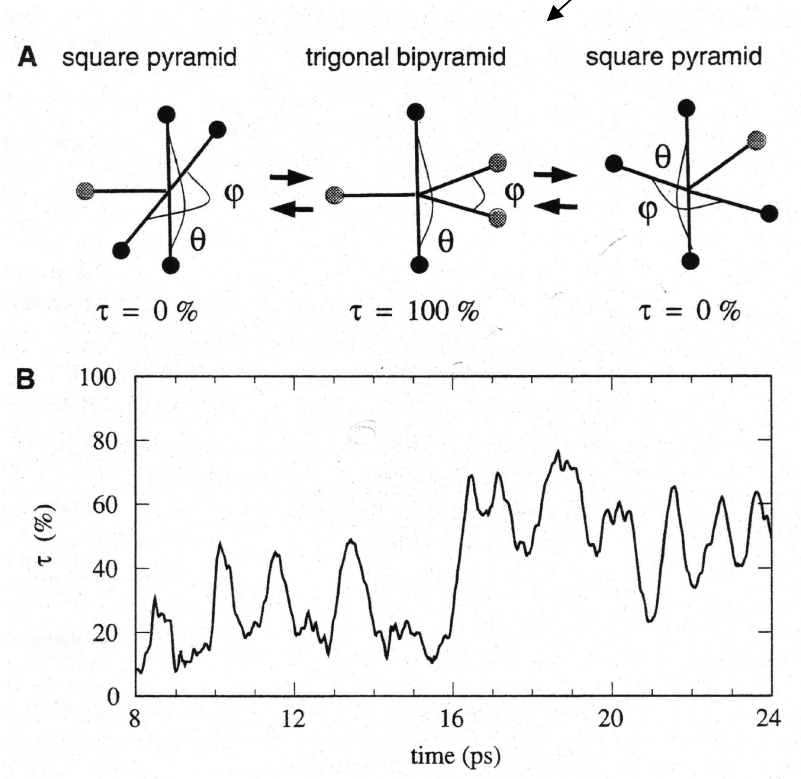

GNXAS analysis

0.1 M Cu^{2+} water solution
H atoms are included

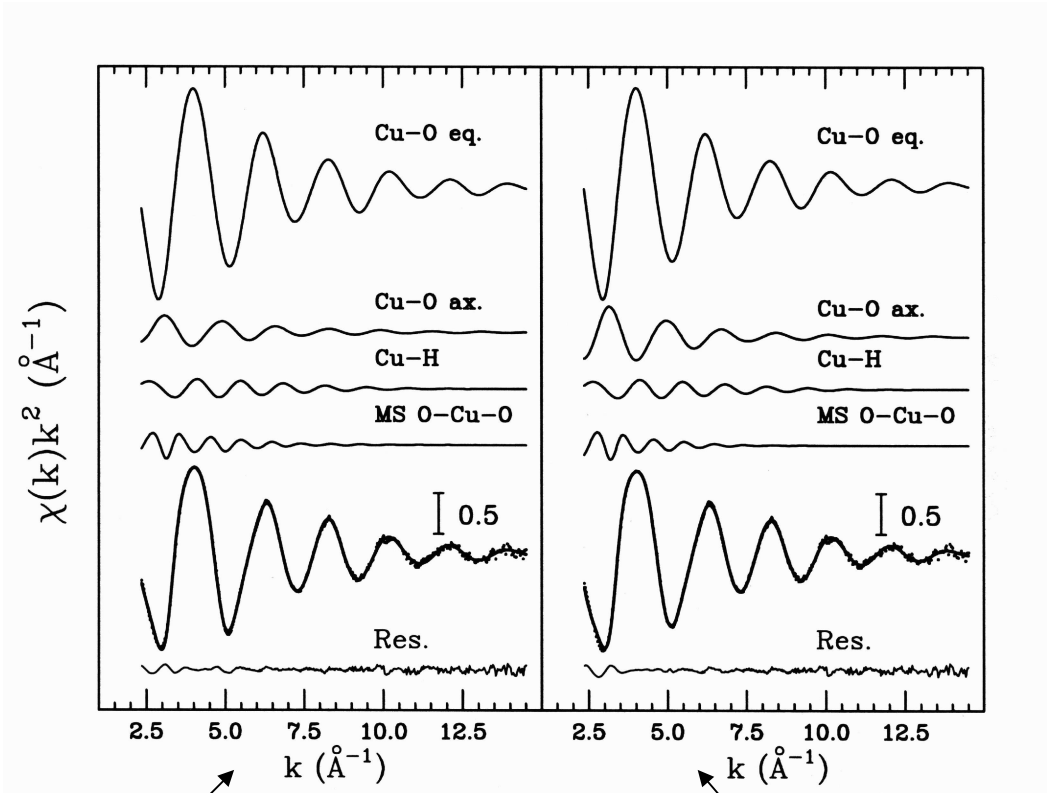

Fivefold coordination

sixfold coordination

Two geometries with the same accuracy

4 equa. O at 1.96 Angs
1 axial O at 2.36 Angs

4 equa. O at 1.96 Angs
2 axial O at 2.36 Angs

MXAN analysis

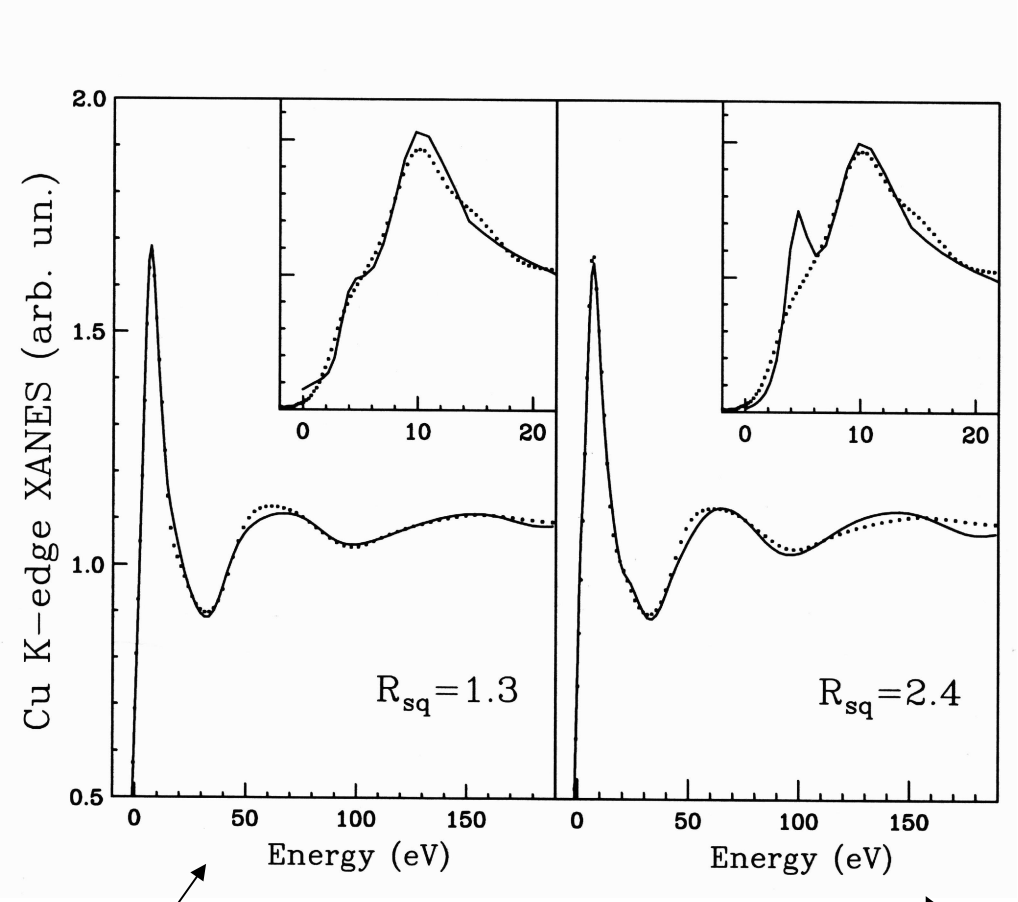

Fivefold coordination

sixfold coordination

Two different solutions

4 equa. O at 1.97(1) Angs
1 axial O at 2.39(6) Angs

4 equa. O at 1.99(1) Angs
2 axial O at 2.56(4) Angs

Combining the two possible solutions

An average fivefold coordination geometry

	N	R	σ^2
Cu-$O_{eq.}$	4	1.956(4)	0.0053(5)
Cu-$O_{ax.}$	1	2.36(2)	0.010(3)

A possible dynamic picture

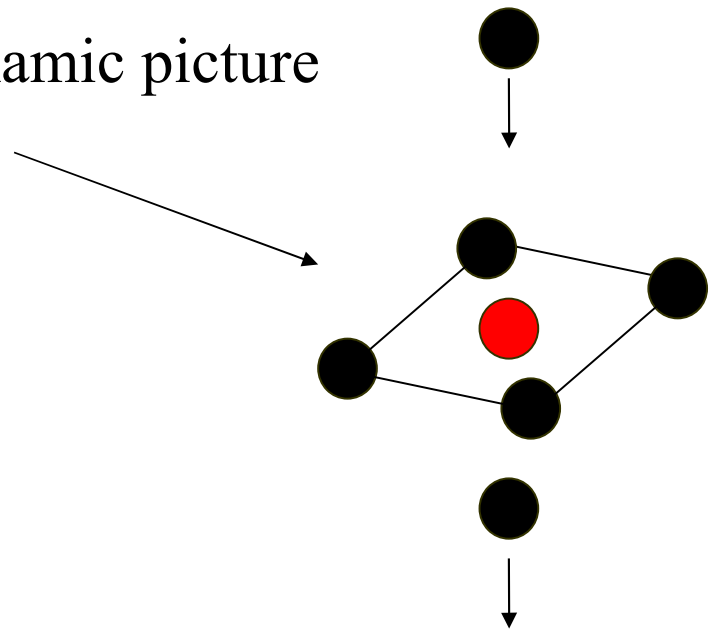

Comparison with neutron diffraction

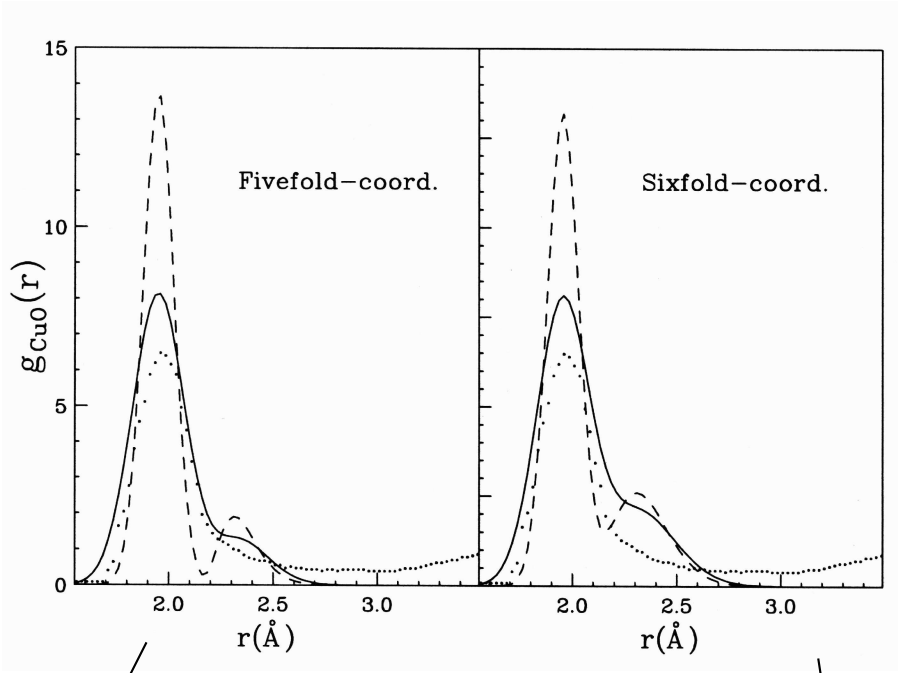

	N	R	σ^2
Cu-O$_{eq.}$	4	1.956(4)	0.0053(5)
Cu-O$_{ax.}$	1	2.36(2)	0.010(3)

	N	R	σ^2
Cu-O$_{eq.}$	4	1.961(4)	0.0058(5)
Cu-O$_{ax.}$	2	2.36(2)	0.020(3)

Sperm whale myoglobin single crystal

Space group $P2_1$

Unit cell data

a = 64.18 Å

b = 30.84 Å

c = 34.69 Å

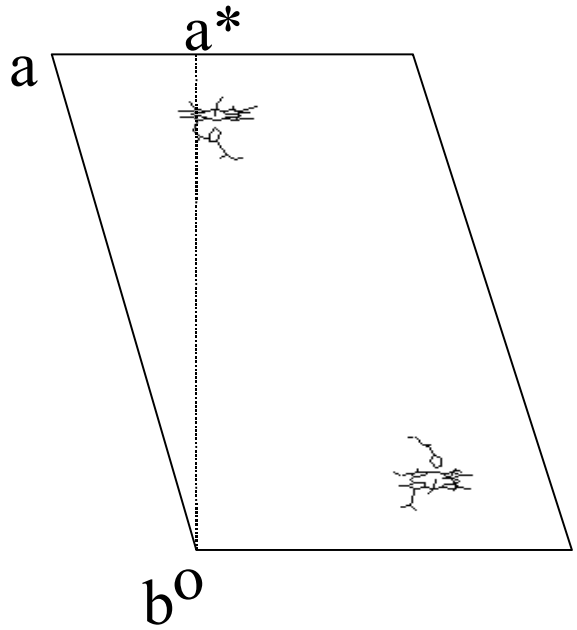

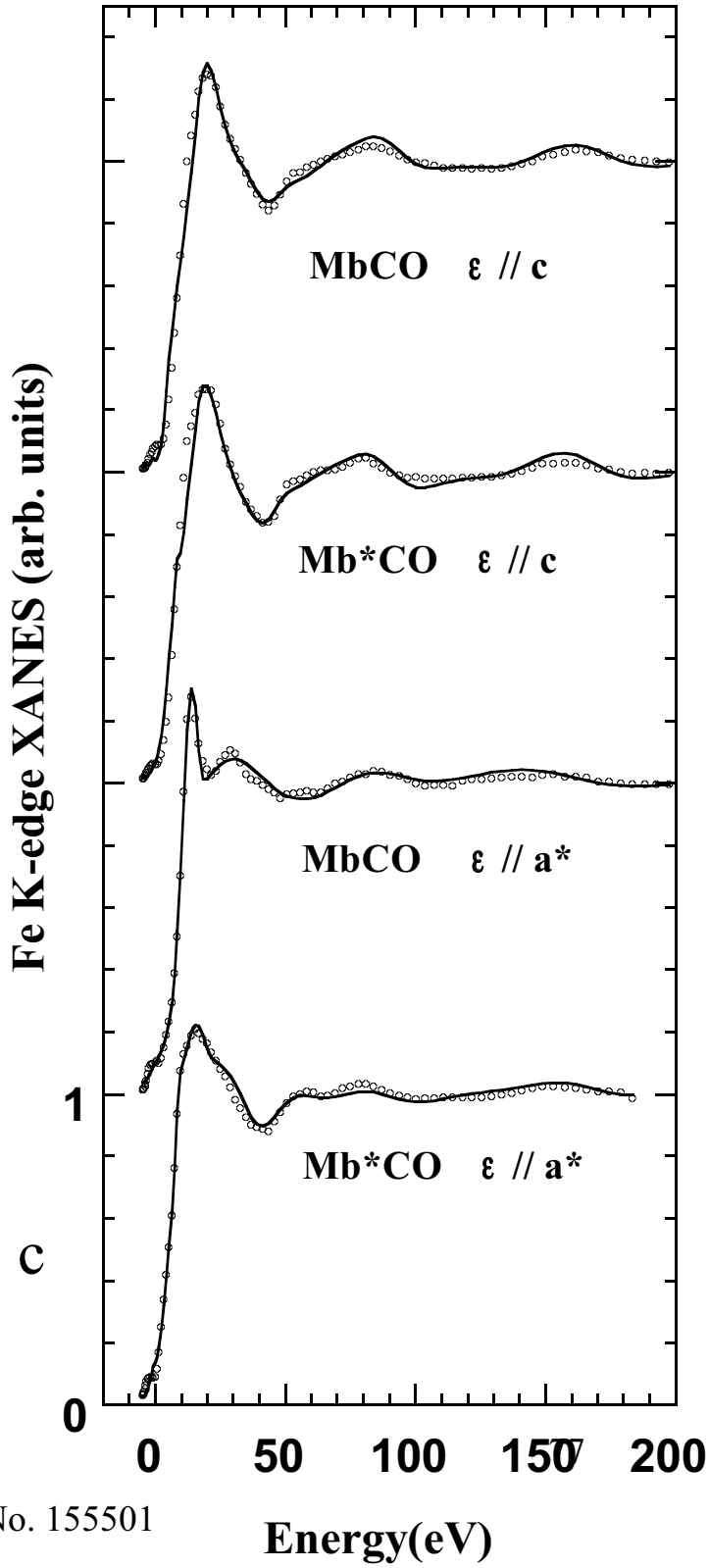

S. Della Longa et al. PRL (2001), **87** Art. No. 155501

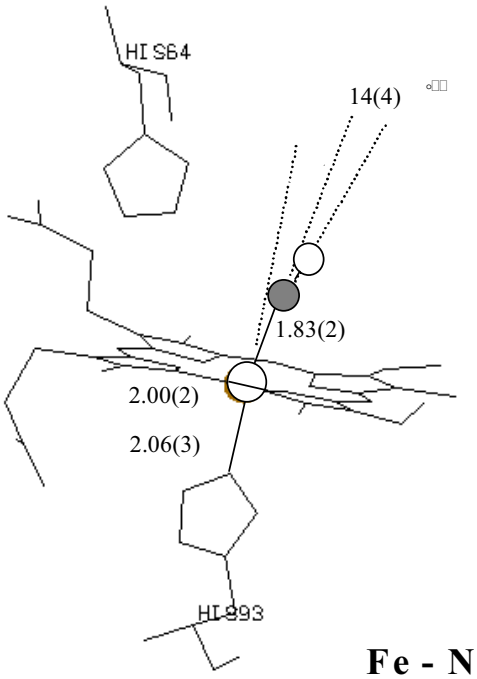

MbCO

	Fe - Np	Fe - Nhis	Fe - C	α	β	C - O
1MBC 1.5Å	1.97	2.19	1.92	3	38	1.17
1BZR 1.1Å	1.98	2.06	1.73	4	7	1.12
1A6G 1.1Å	1.98	2.06	1.82	9	9	1.09
MXAN fit	2.00(2)	2.06(3)	1.83(2)	--	14(4)	1.07

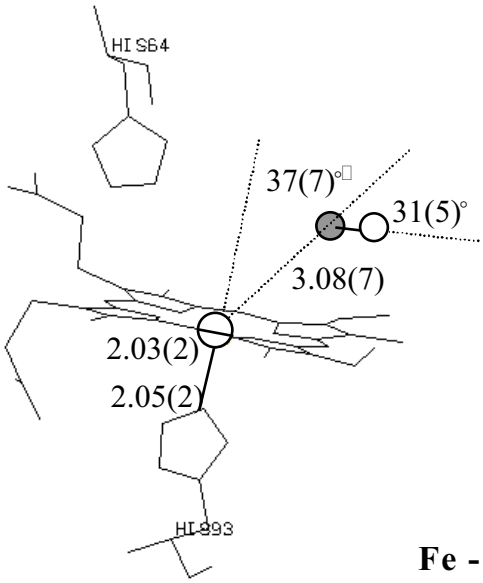

Mb*CO

	Fe - Np	Fe - Nhis	Fe - C	α	β	C - O
1AJH 1.7Å	2.00	2.11	2.84	23	45	1.21
1ABS 1.5Å	1.97	2.25	3.60*	27*	54	1.12
MXAN fit	2.03(2)	2.05(2)	3.08(7)	37(7)	31(5)	1.24

High XANES sensitivity to the CO position

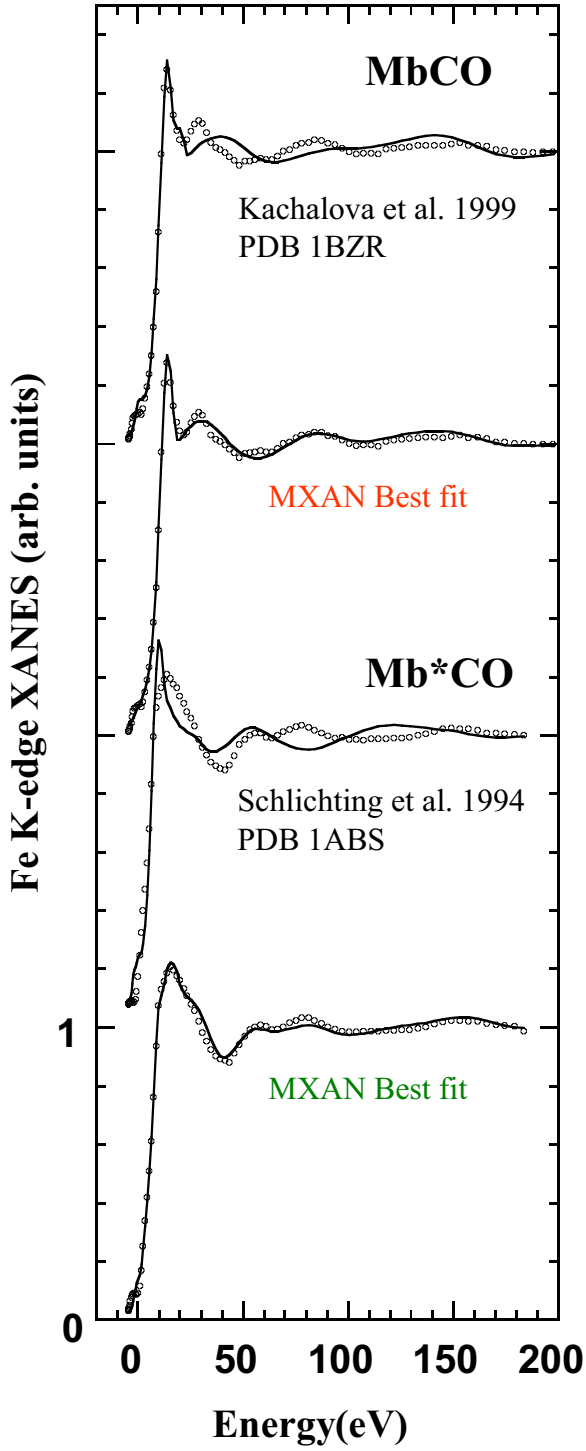

Several applications

From the coordination geometry of metal site in proteins to the local structure of Mn in manganite

S. Della Longa et al. Biophy. Jour. (2003) **85**, 549
P. Frank et al. Inorganic Chemistry (2005) **44**, 1922
C Monesi et al. PRB **72**, 174104 (2005)
R. Sarangi et al. Inorganic Chemistry (2005) **44**, 9652
P. D'Angelo et al. JACS (2006) **128**, 1853

Recently we have modified MXAN to analyze the difference spectrum

$$\Delta A(E,\Delta t) = f(\Delta t)[\mu_{ex}(E,\Delta t) - \mu_{gs}(E)]$$

$f(\Delta t) \longleftarrow$ is the fractional population of the ex state at time delay Δt

To see (small) structural changes due to physical/chemical reasons in pump-probe experiments

Fields of application:

time resolved experiment
changes of chemical-physical and/or thermo-dynamical conditions
……

M. Benfatto et al. J. Phys. Chem. B (2006), **110** 14035

Two applications

ruthenium (II) tris-2,2'-bypyridine

the Ru^{II} to Ru^{III} transition

iron-(II)-tris-bypyridine $[Fe^{II}(byp)_3]^{2+}$

from LS to HS state

The case of iron-(II)-tris-bypyridine $[Fe^{II}(byp)_3]^{2+}$

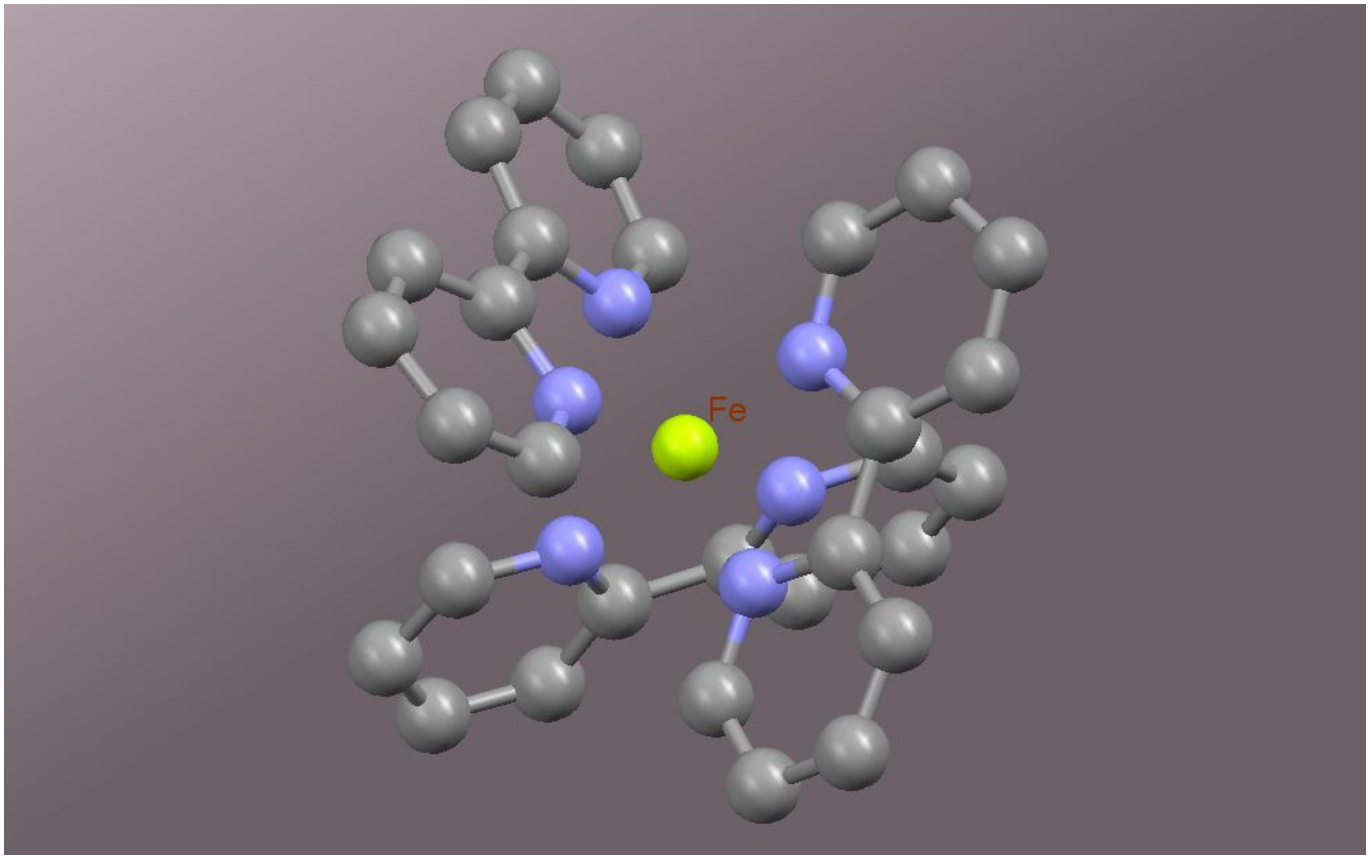

see the structural changes going from LS to HS state

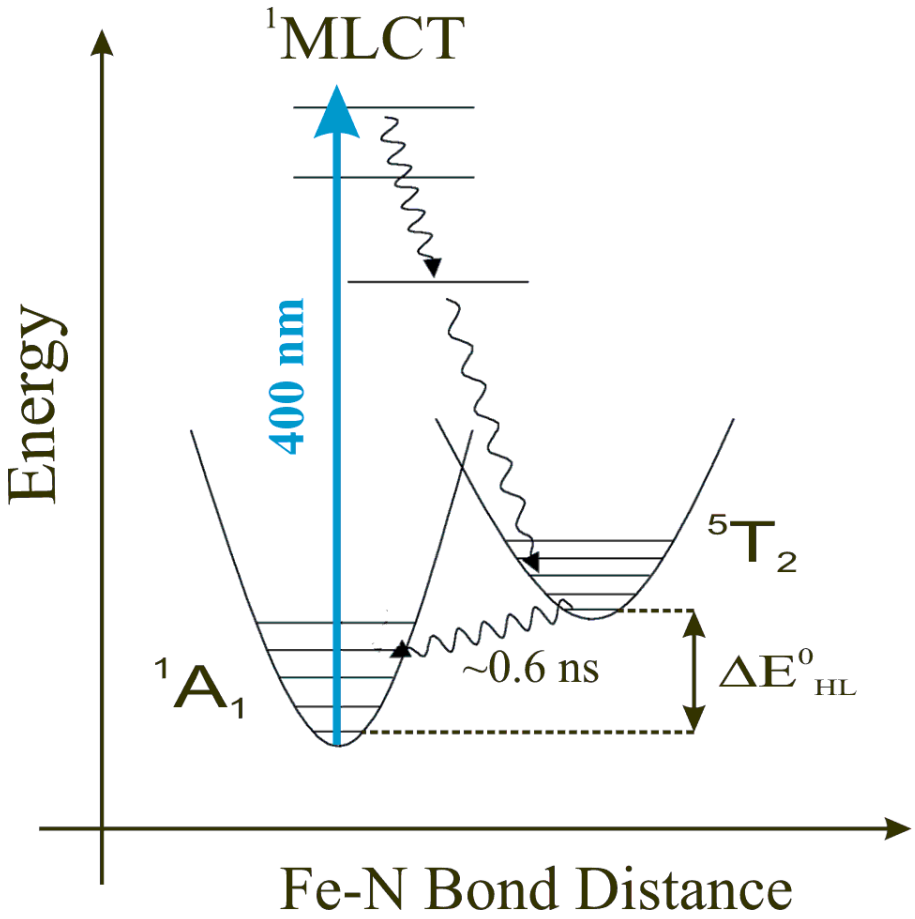

experiment done at the micro-XAS line of SLS by Chergui's group - pump-probe experiment in aqueous solution and room temperature

The detected signal is directly the quantity $\Delta A(E,\Delta t)$

experimental data

HS exs transient data at Δt = 50 ps

LS gs data

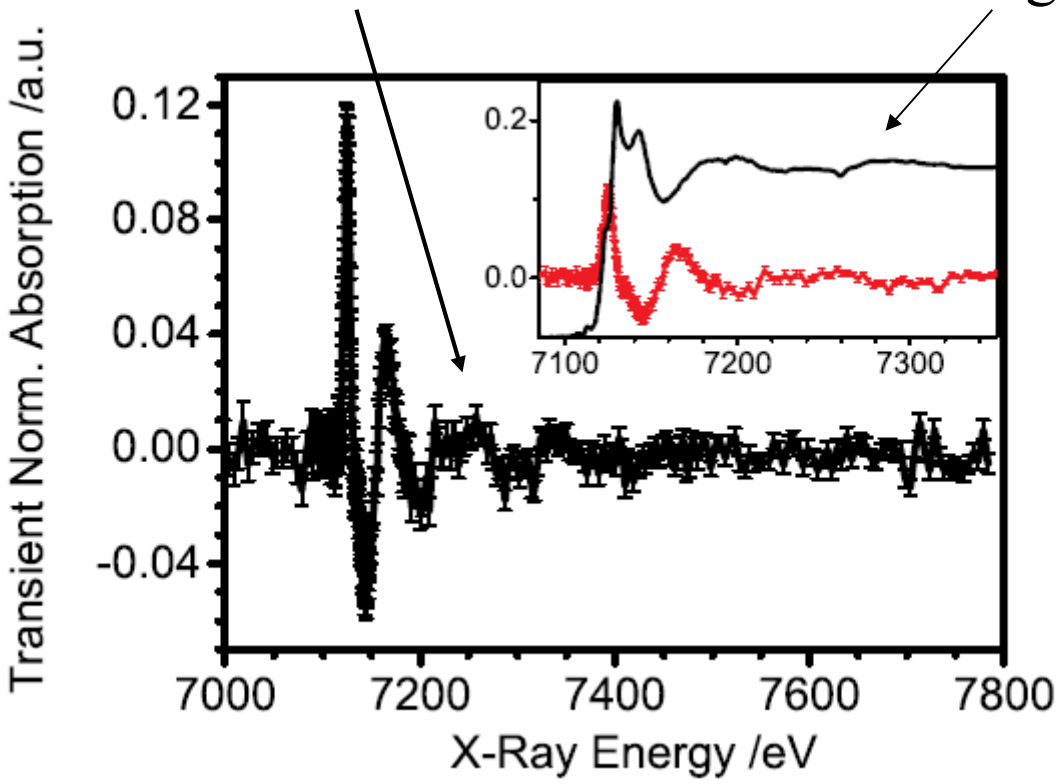

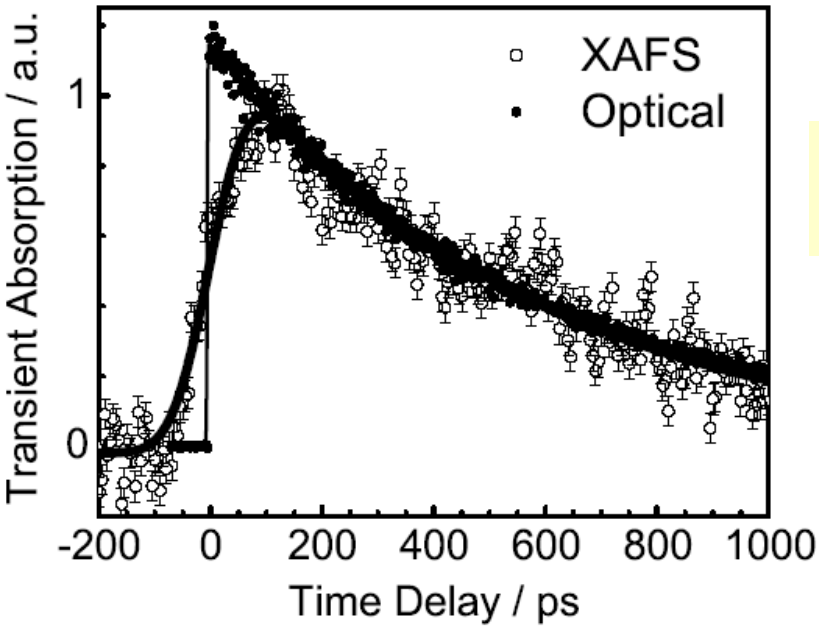

Kinetics of transient XAS and optical signals

LS ground state fit

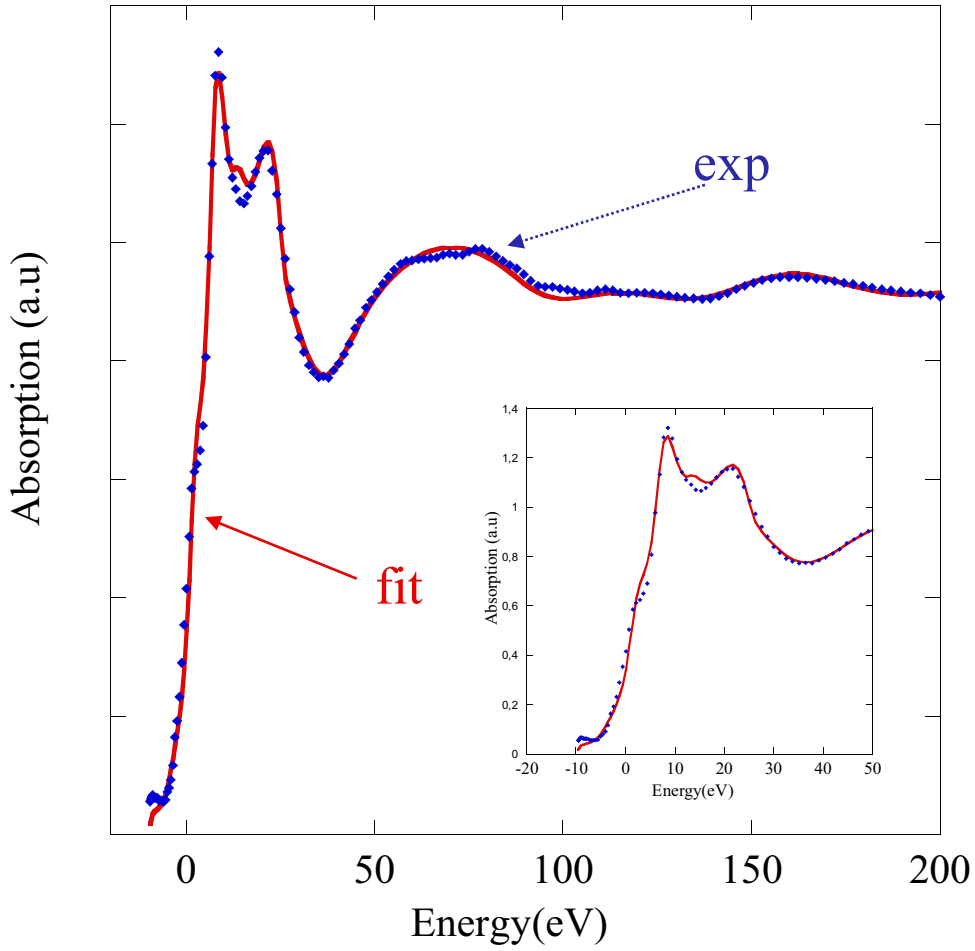

$R_{Fe\text{-}N} = 2.00 \pm 0.02$ Å

$R_{Fe\text{-}N} = 1.967 \pm 0.006$ Å (XRD)

$R_{Fe\text{-}N} = 1.99 \pm 0.02$ Å (DFT)

HS excited state fit by transient data

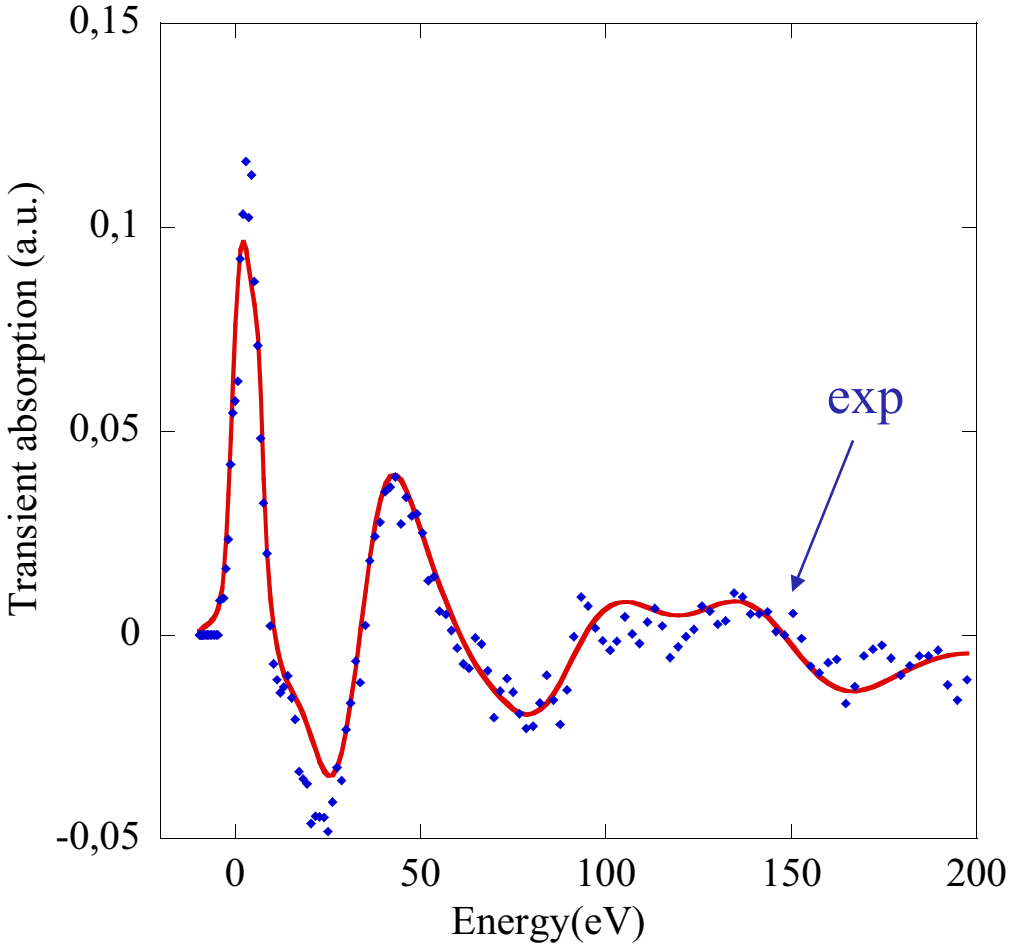

supposing a chemical shift $\Delta E = -2.5 \pm 0.5$ eV

$\Delta R_{Fe\text{-}N} = 0.20 \pm 0.05$ Å

DFT calculations indicate ~ 0.2 Å

W. Gawelda et al. PRL (2007) **98**, 057401

We can also derive more information

$$\sigma_{gs}(E) = N_0 \mu_{gs}(E)$$

$$\sigma_{exs}(E) = N_0 \mu_{exs}(E)$$

N_0 is the constant value that transforms the cross section to absorption coefficient - we suppose it is the same for both exs and gs states

For transient data

$$\sigma_{exc}(E) - \sigma_{gs}(E) = N_1 \Delta A(E) =$$

$$N_0[\mu_{exs}(E) - \mu_{gs}(E)]$$

$f = N_0 / N_1$ We can obtain the fractional population

N_0 and N_1 come from the MXAN analysis

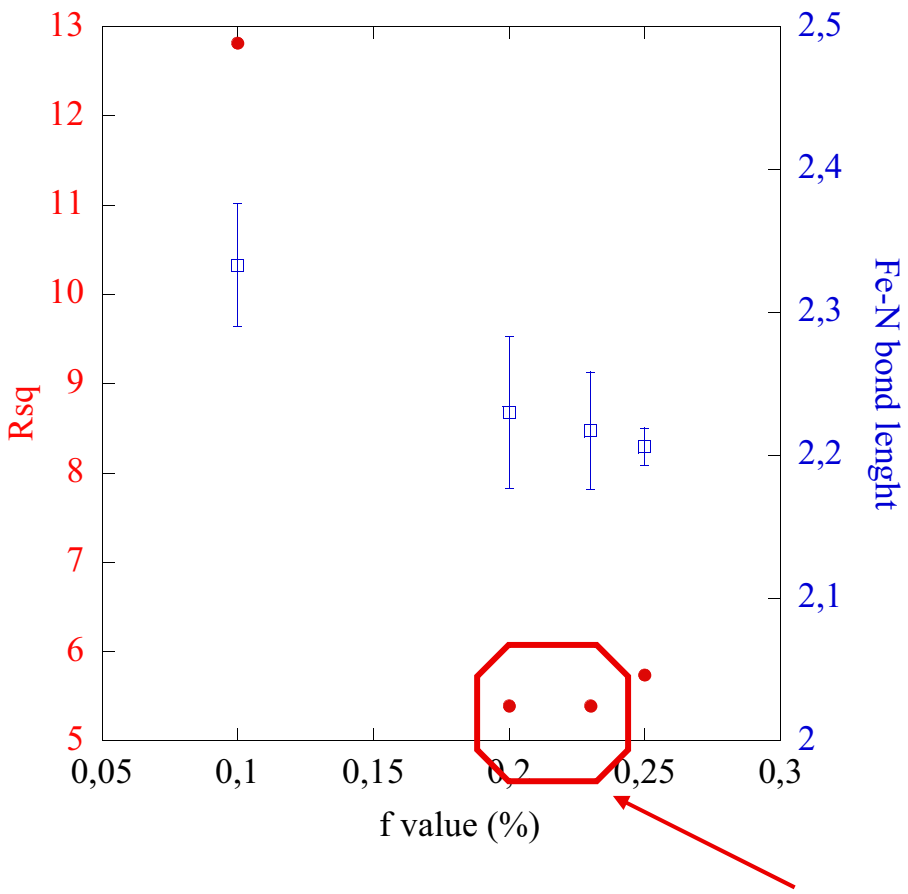

minimum at 20-23 %

optical measurement gives 22 ± 2 % at Δt=50 ps

a similar type of analysis can be done to get the chemical shift

thermal and structural disorder

We use MD to generate thousands of geometrical configurations – each snapshot with a time step of 50 fs is used to generated one XANES spectrum – average using ~ 10^4 geometrical configuration

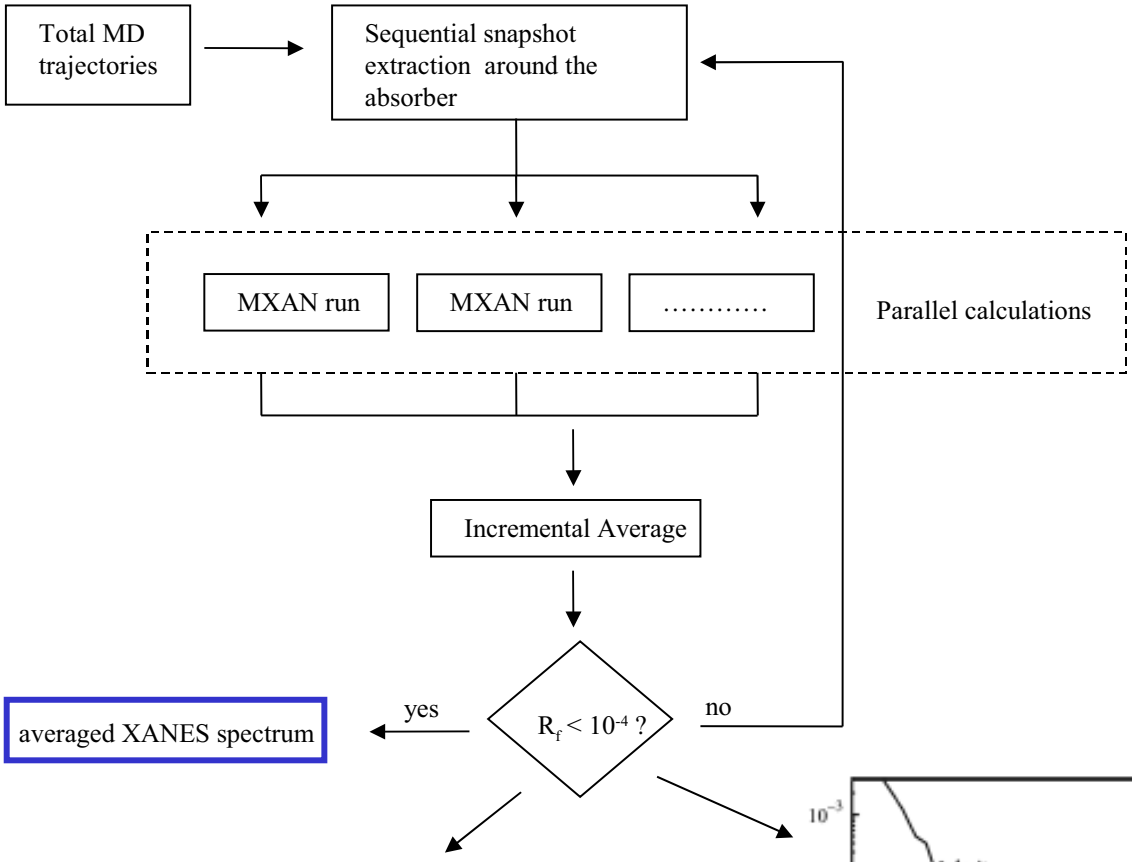

$$R_f(N) = \left[\sum_i [\sigma^N(E_i) - \sigma^{N-1}(E_i)]^2 \right]^{1/2}$$

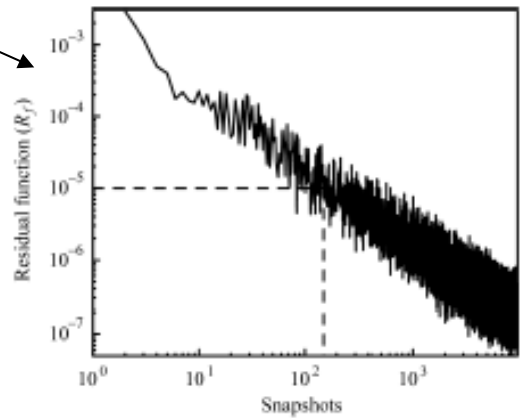

Merkling et al. JACS **124** (2002)
Campbell et al. Jour.Synch.Rad. **6** (1999)

Ni^{2+} in water – Ni Kedge

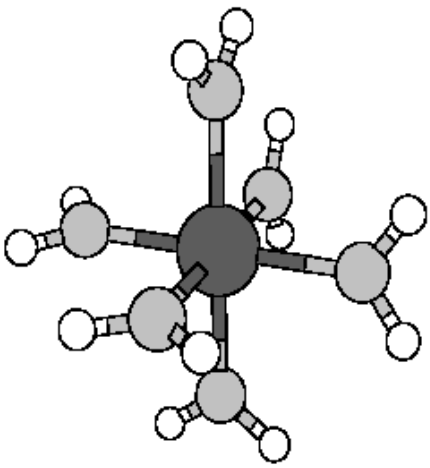

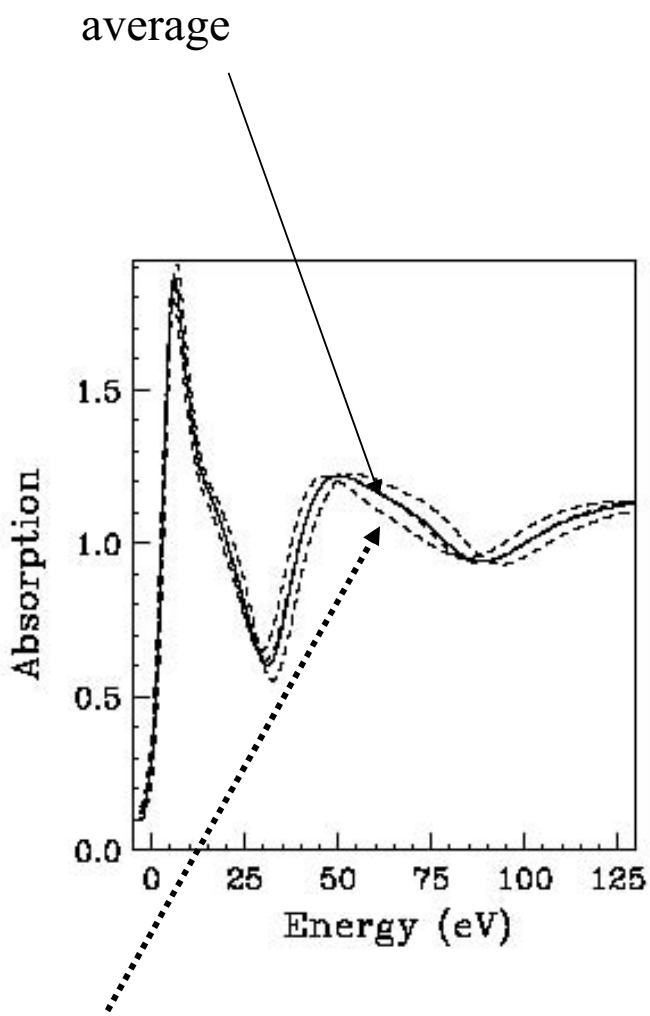

Calculations for some particular snapshots

Comparison between the averaged theoretical spectrum and a single theoretical spectrum at the symmetrical first shell configuration

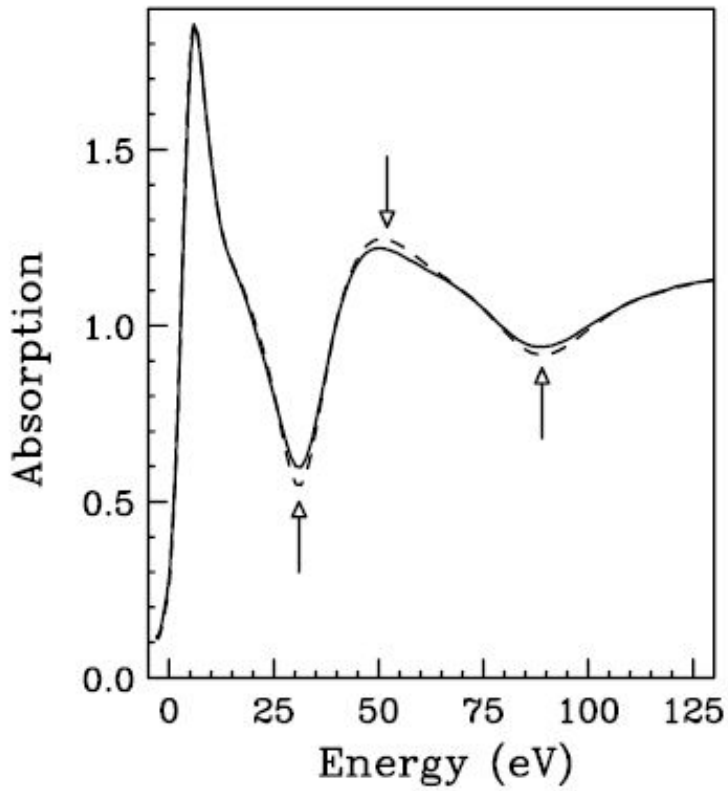

Arrows indicate the damping - very weak effect - it can be included in the phenomenological treatment of the inelastic losses in MXAN

including the second shell

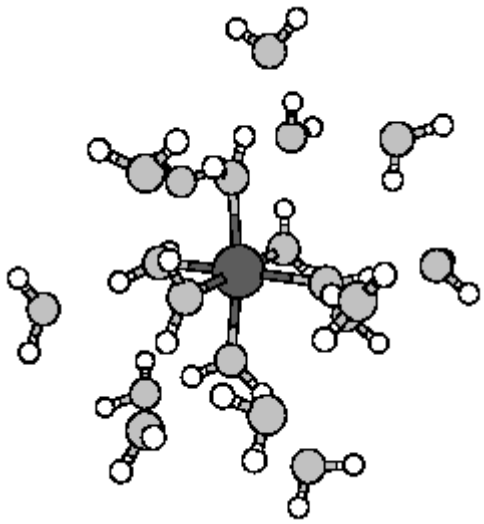

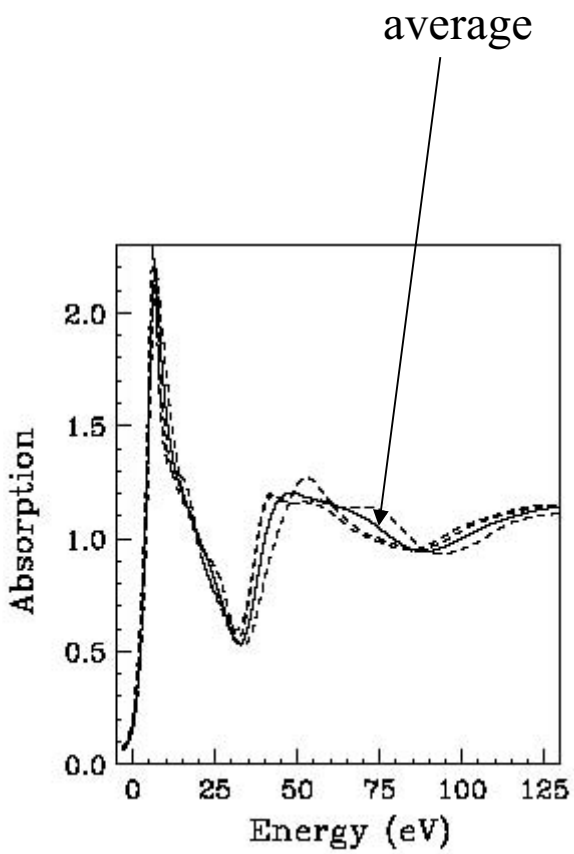

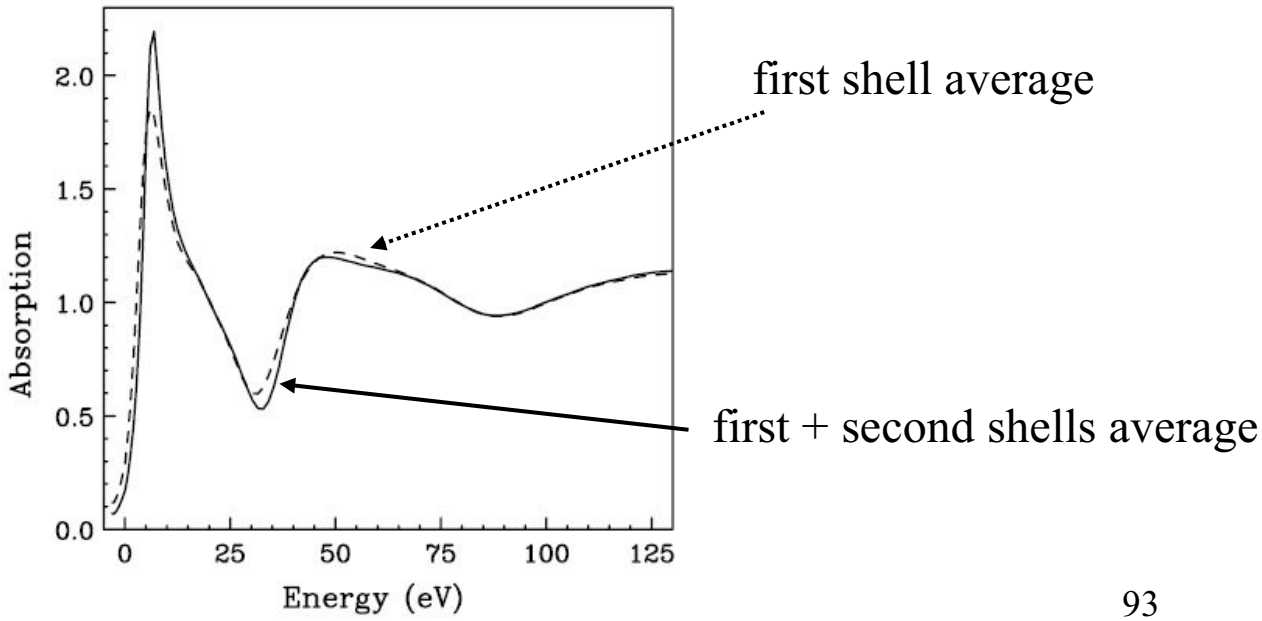

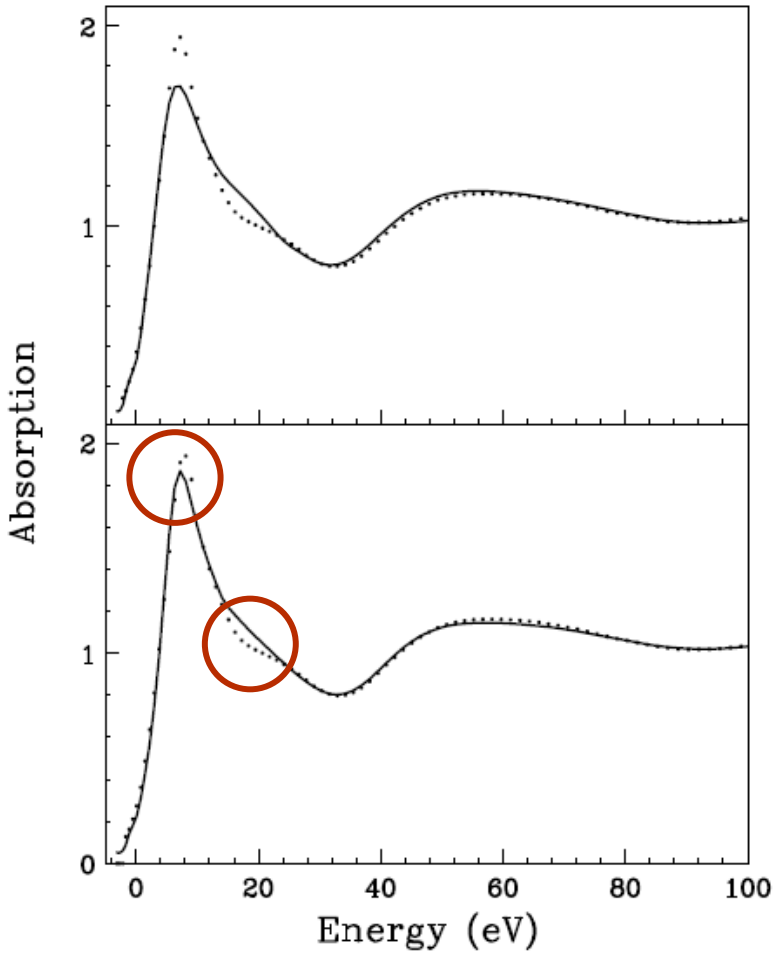

one shell fit

two shells fit

sizeable effects in the energy range 0 - 30 eV

P. D'Angelo et al. JACS **128** (2006)

The water solvation of I^-

L1 - L3 XAS data

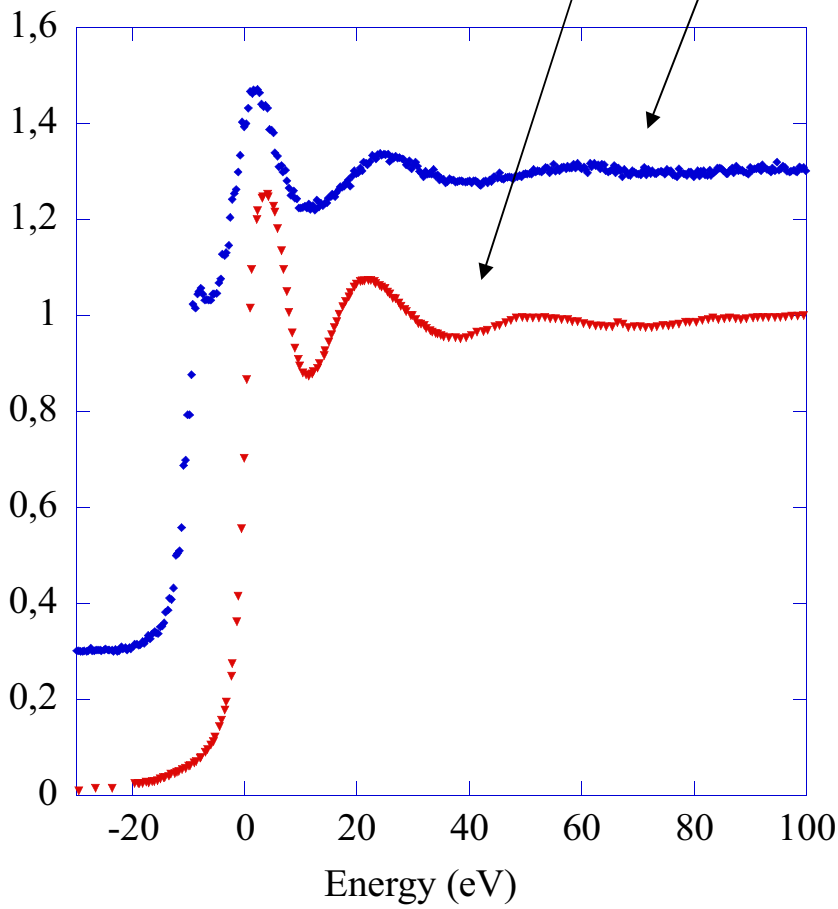

as in the previous case we analyze those data by MD snapshots generate by QM/MM and DFT methods

in collaboration with Chergui's group

I-O pair distribution function from MD

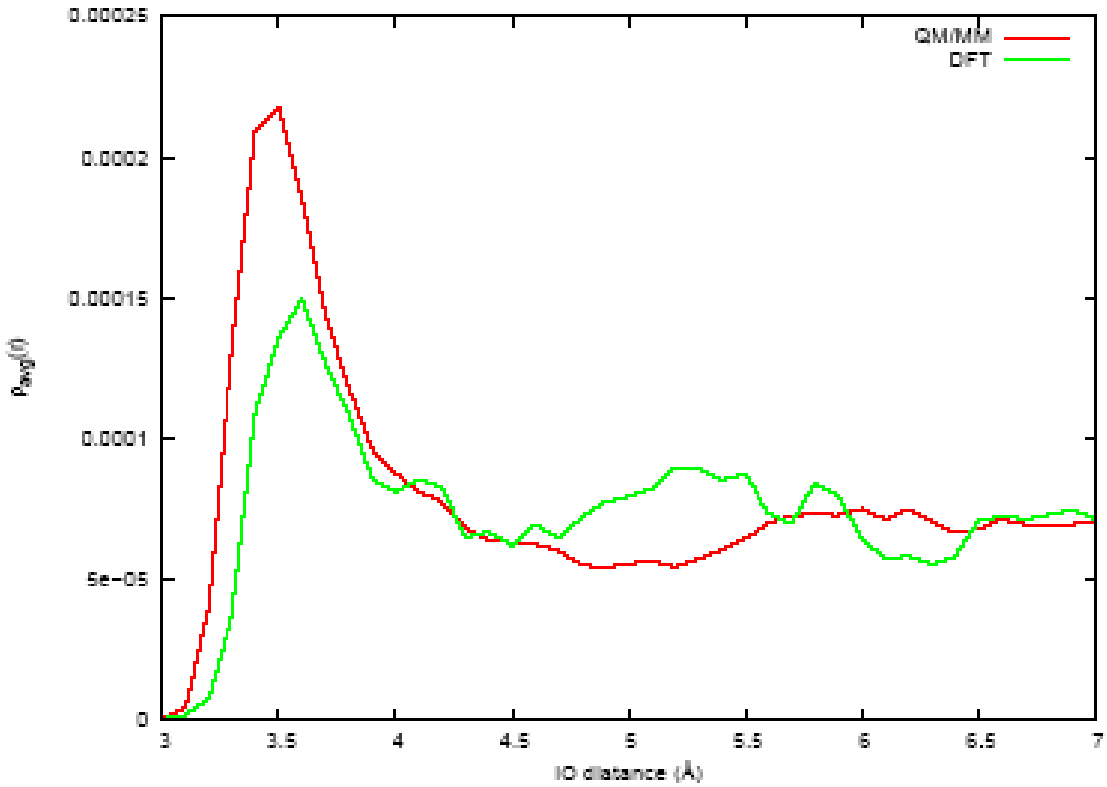

the calculated coordination number varies from 7 to 9.7 - difficulty to define a solvation shell

We have used more than 1000 frames - three of them at L3 edge

The calculation includes atoms (H and O) up to 7 Å

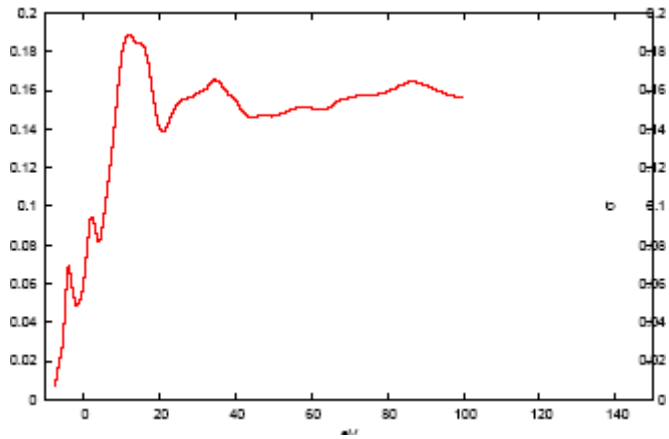

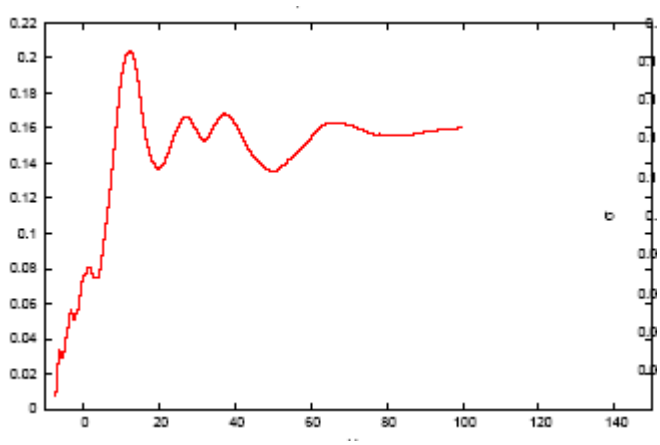

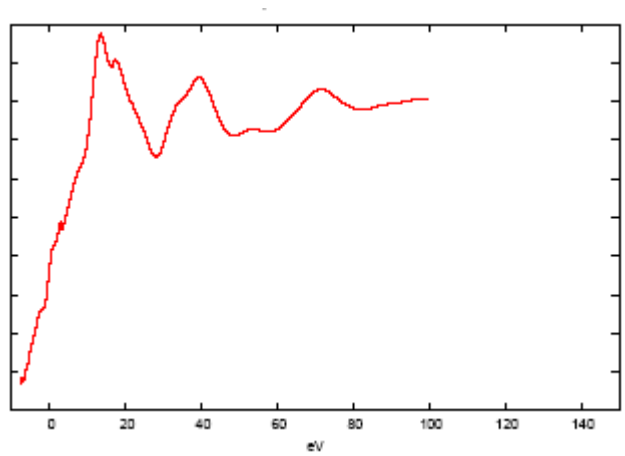

Very disordered system!

L1 Fits

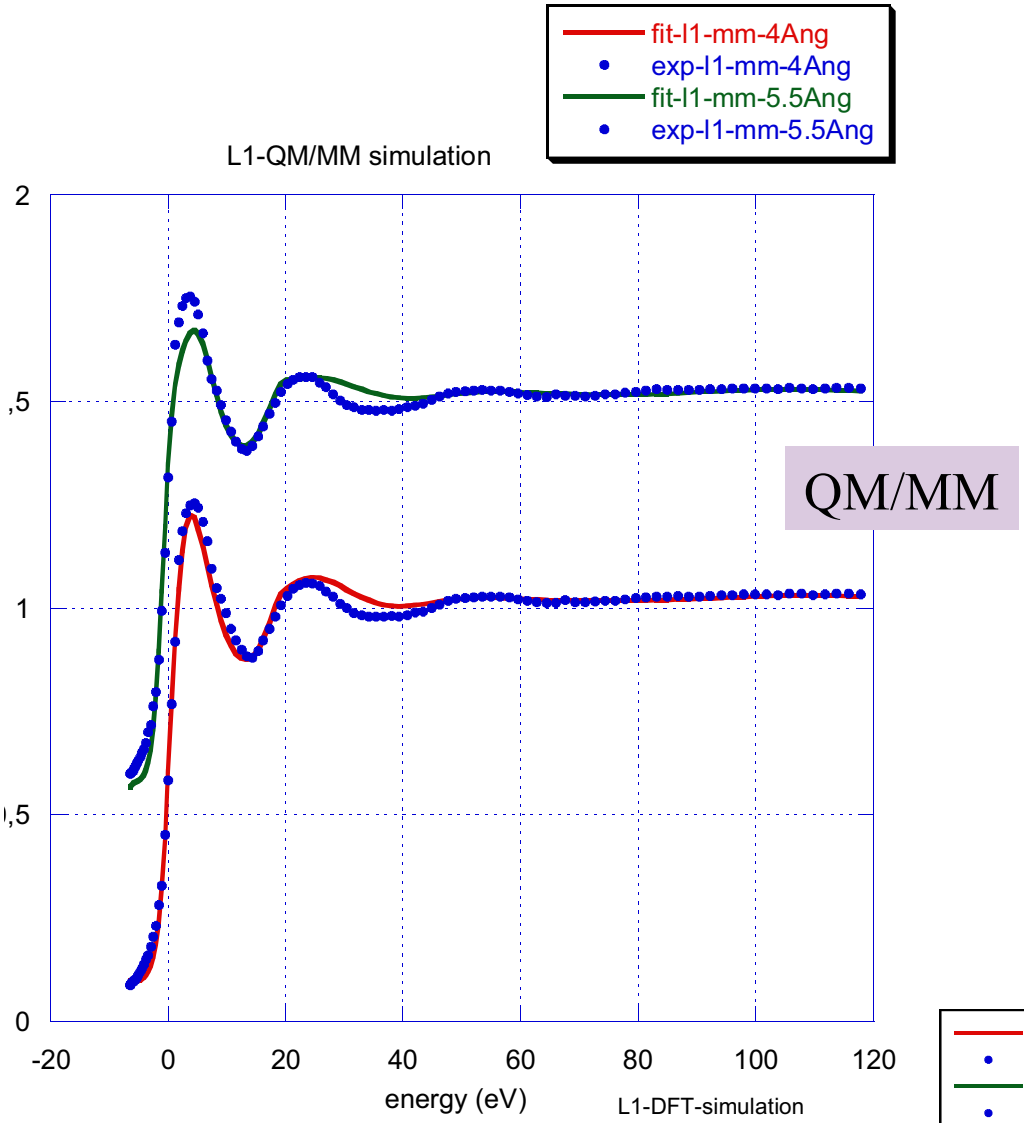

QM/MM

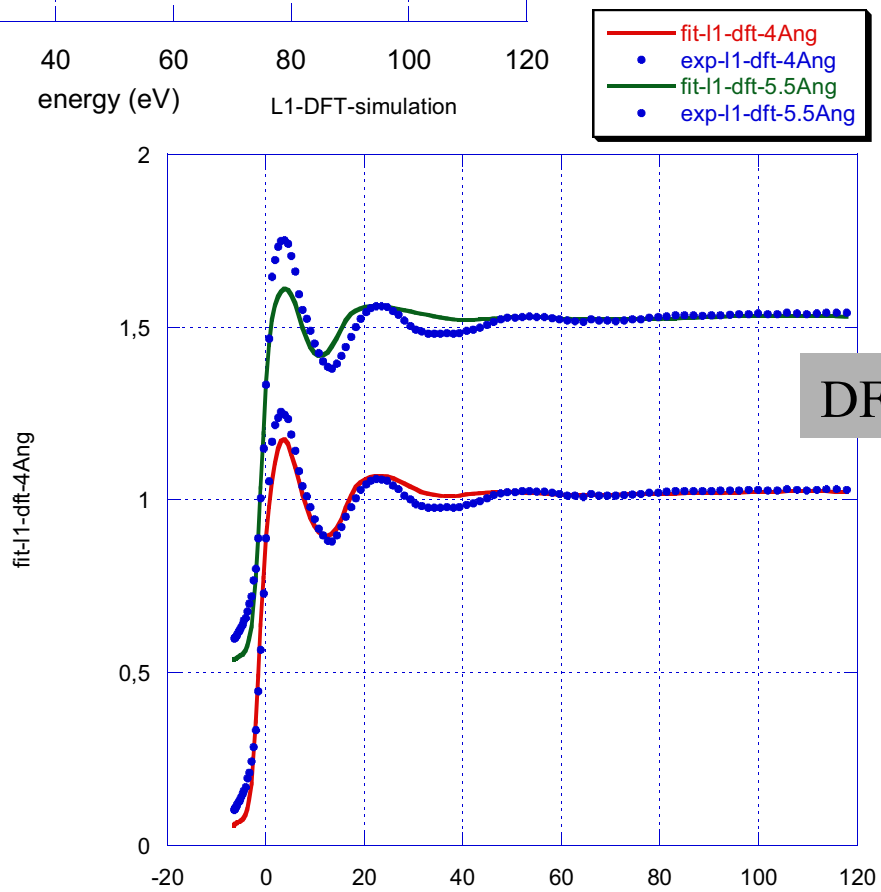

DFT

The QM/MM calculations reproduces better than DFT the experimental data for both L1 and L3 edges - Increasing the cluster size DFT becomes worse than QM/MM

It seems that DFT introduces a partial order that is not verify in the reality

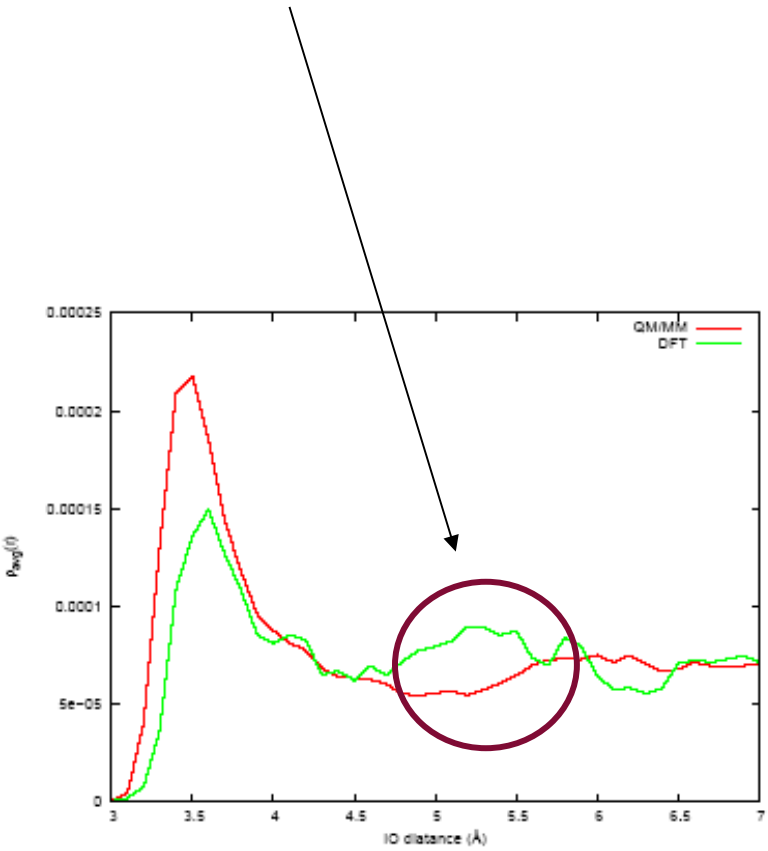

L3 Fits

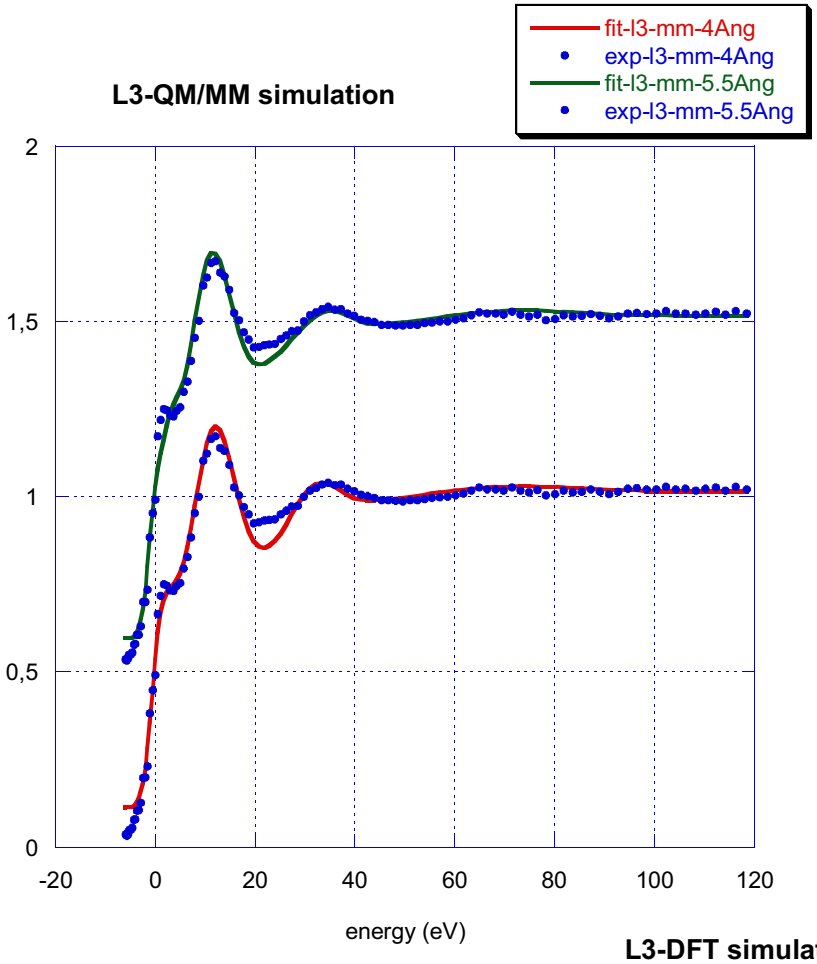

QM/MM

DFT

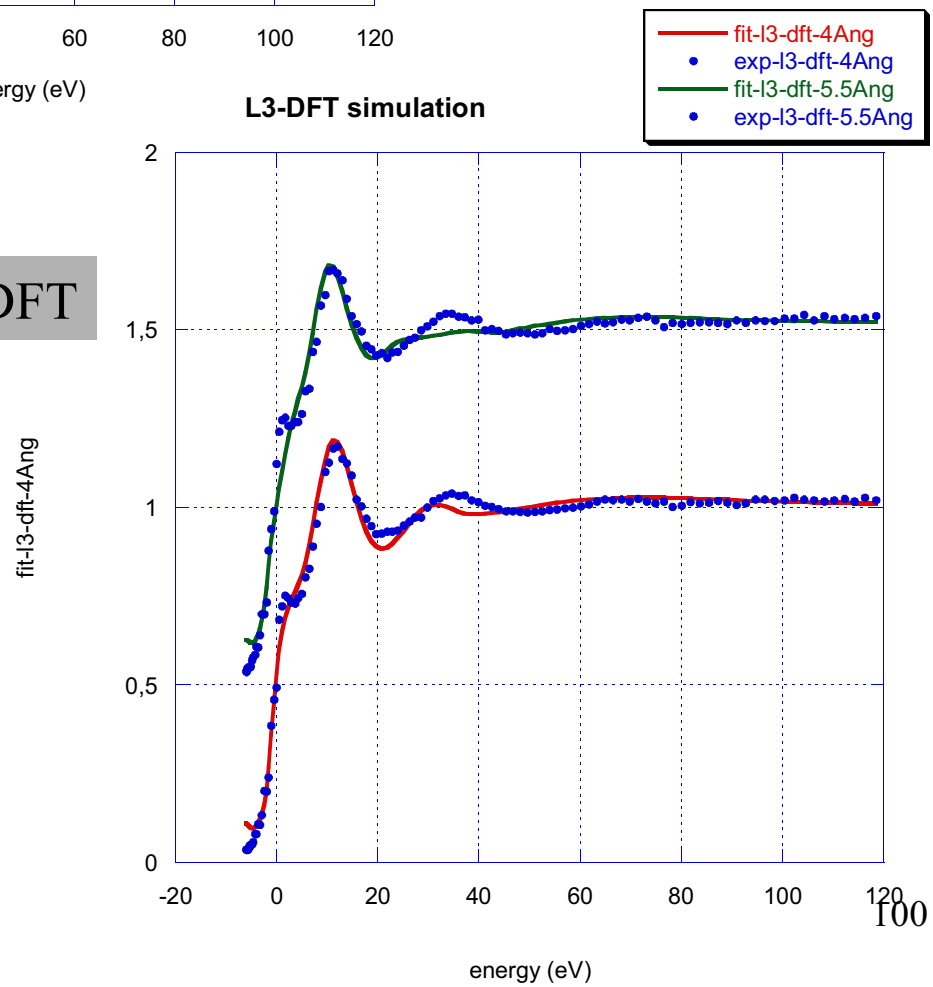

The role of the non-MT corrections in the structural fitting

Ni^{2+} in water – Ni Kedge

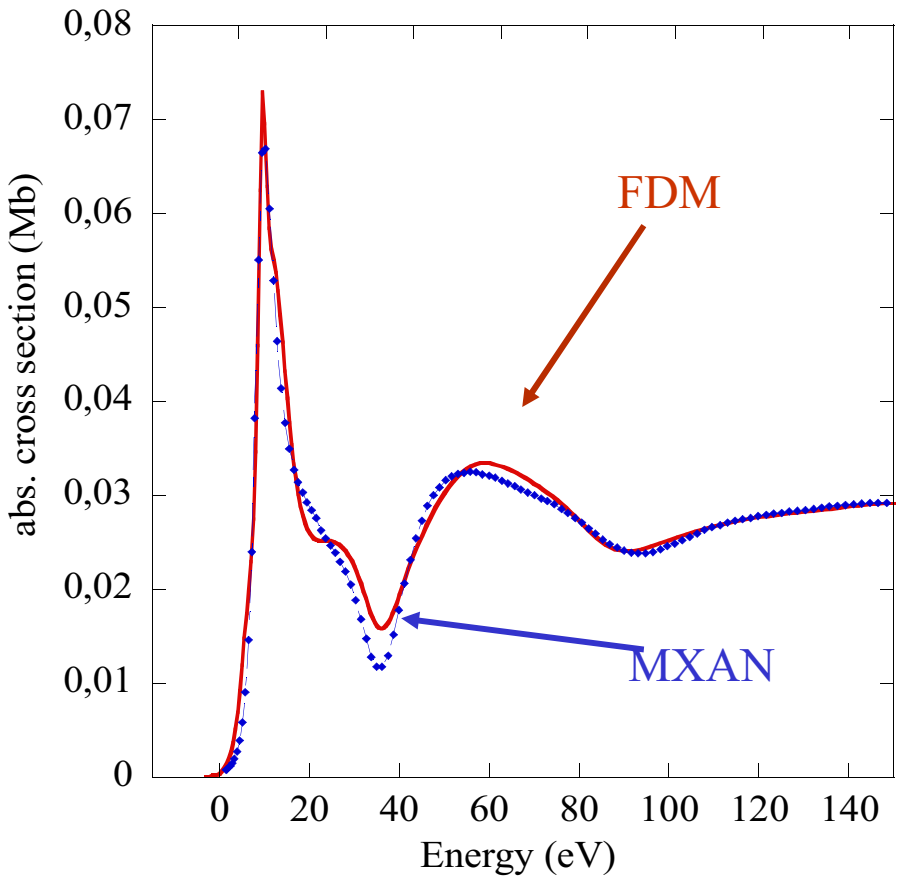

calculations without any damping at the MXAN best fit structural determination - H atoms are included

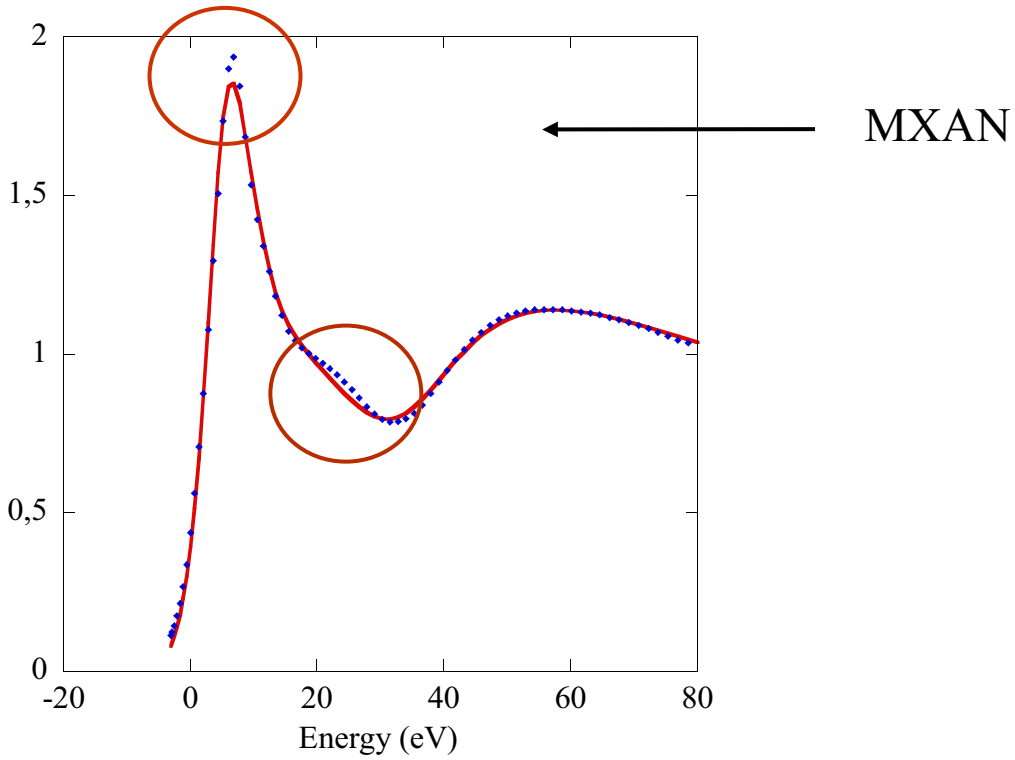

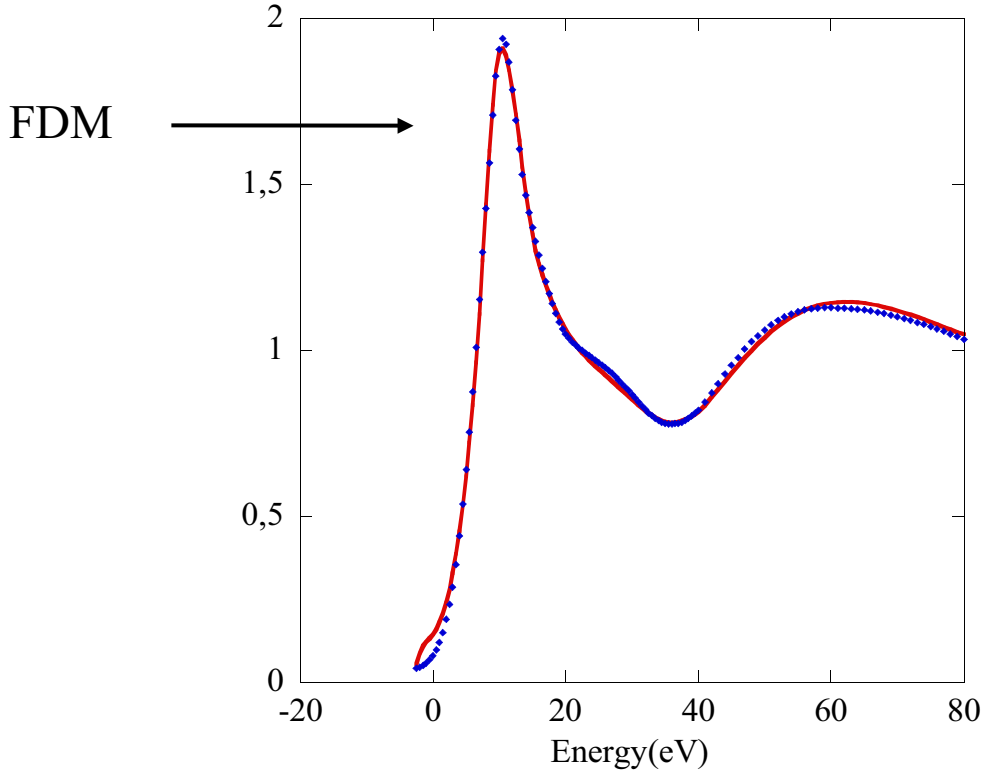

we have used the same geometry obtained by MXAN

behavior of the Rsq as function of Ni-O distance

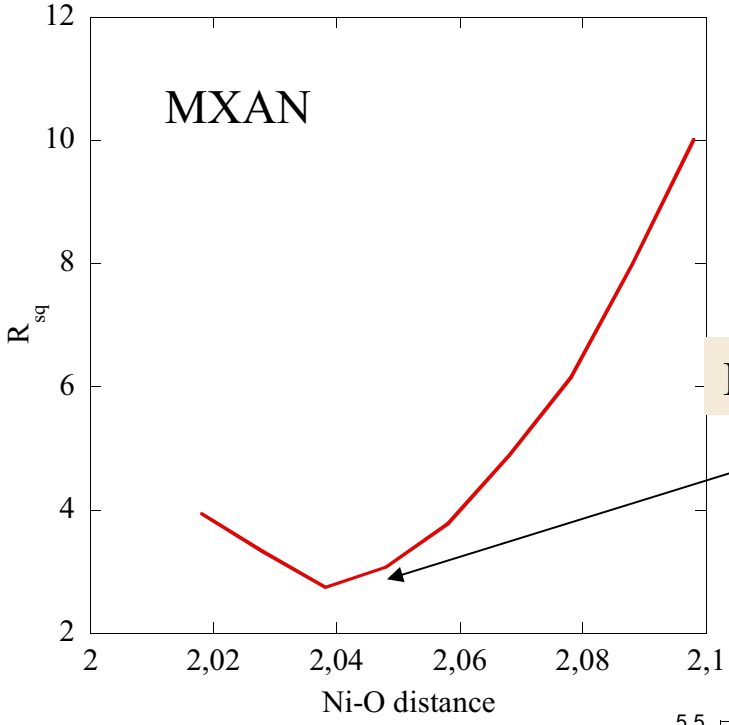

Rsq = 2.75 → d(Ni-O)=2.038

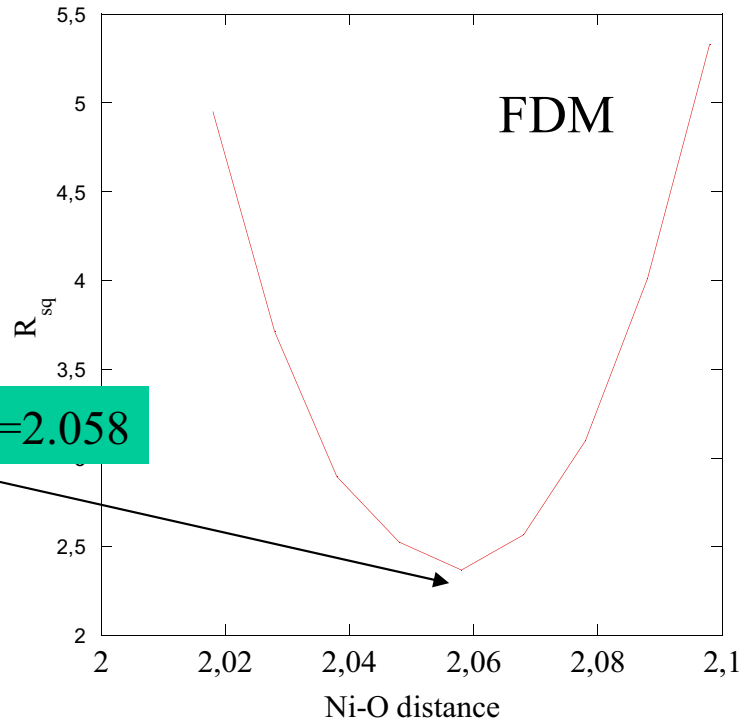

Rsq = 2.37 → d(Ni-O)=2.058

The best EXAFS determination gives d(Ni-O)=2.072

The role of the MT approximation

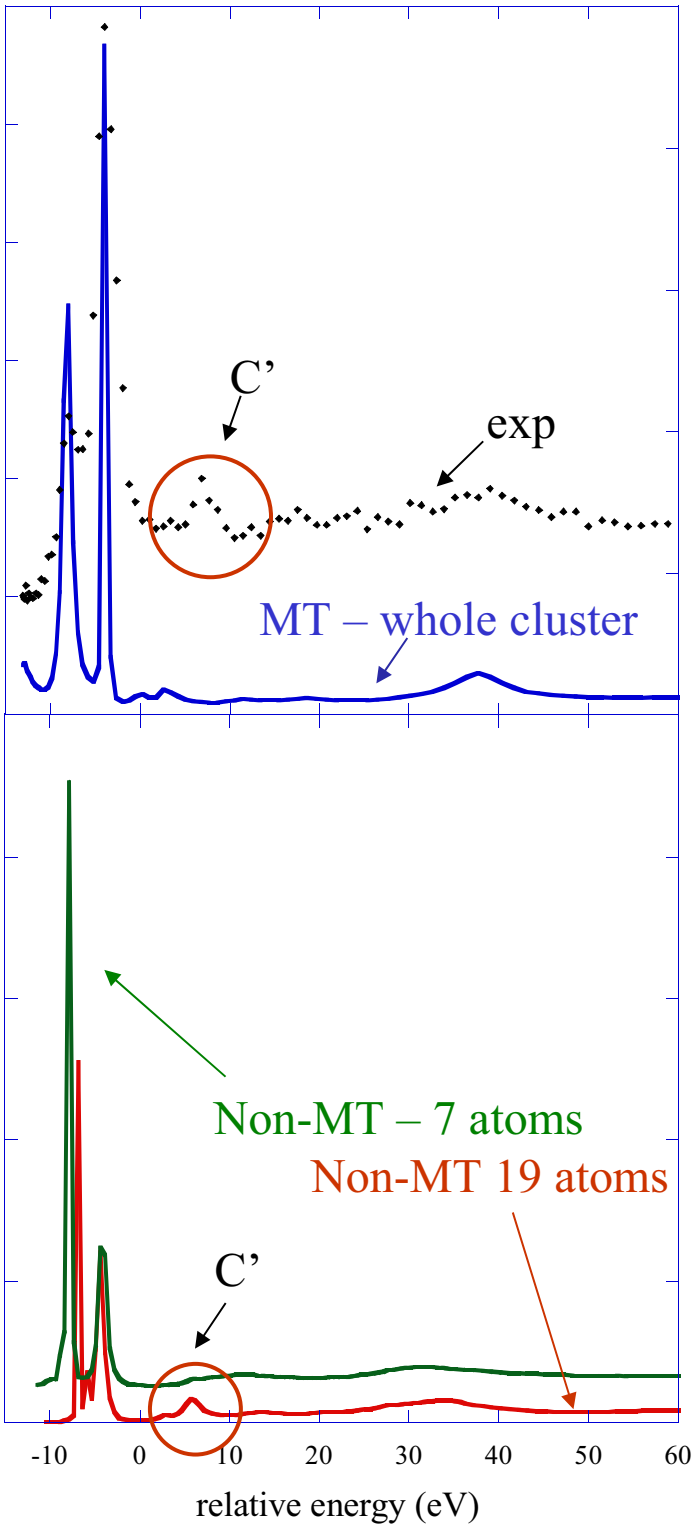

Real calculation without any inelastic losses

FDM method

C' feature appears only when the cluster size is big enough – in the MT calculation is very weak

The improvement in the structural determination is small - This type of behavior is quite common - small changes in the first 20-40 eV with weak effects in the structural fit.

We note that it is always possible to write a non-MT theory as

$$\sigma_t \approx \mathrm{Im}(T + H)^{-1}$$

$$T = (T_a)^{-1} + \Delta T$$

$$H = H_{MT} + \Delta H$$

$$\sigma_t \approx \mathrm{Im}\left\{ \sum_{n=0} (-1)^n [(T_a^{-1} + H_{MT})^{-1} \Delta]^n (T_a^{-1} + H_{MT})^{-1} \right\}$$

$$\Delta = \Delta T + \Delta H$$

$$\sigma_t \approx \sigma_{MT} + corr(E; V_{\mathrm{int}})$$

C.R. Natoli, M.Benfatto and S. Doniach PRA **34**, (1986)
M. Benfatto and S. Della Longa Journal of Sync. Rad. **8**, (2001)
R. Sarangi et al. Inorganic Chemistry 44, (2005)

conclusions

- The geometrical arrangement essentially dominates the XAS spectroscopy in the whole energy region

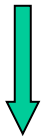

- Now it is possible to fit the XANES energy range starting from the edge to obtain quantitative structural information

Of course there is still some problems to be solved!

references

General and fitting methods

Tyson TA, Hodgson KO, Natoli CR, Benfatto M, “general multiple-scattering scheme for the computation and interpretation of x-ray-absorption fine-structure in atomic clusters with applications to sf6, gecl4, and br2 molecules”, PHYSICAL REVIEW B 46 (10): 5997-6019, 1992

Filipponi A, DiCicco A,” X-ray-absorption spectroscopy and n-body distribution functions in condensed matter .2. Data analysis and applications”, PHYSICAL REVIEW B 52 (21): 15135-15149, 1995

Binsted N, Hasnain SS, “State-of-the-art analysis of whole X-ray absorption spectra”, JOURNAL OF SYNCHROTRON RADIATION 3: 185-196, 1996

Rehr JJ, Albers RC, “Theoretical approaches to x-ray absorption fine structure”, REVIEWS OF MODERN PHYSICS 72 (3): 621-654, 2000

Natoli CR, Benfatto M, Della Longa S, Hatada K,” X-ray absorption spectroscopy: state-of-the-art analysis”, JOURNAL OF SYNCHROTRON RADIATION 10: 26-42, 2003

Benfatto M, Della Longa S, “Geometrical fitting of experimental xanes spectra by a full multiple-scattering procedure”, JOURNAL OF SYNCHROTRON RADIATION 8: 1087-1094, 2001

Della Longa S, Arcovito A, Girasole M, Hazemann JL, Benfatto M,” Quantitative analysis of x-ray absorption near edge structure data by a full multiple scattering procedure: The Fe-CO geometry in photolyzed carbonmonoxy-myoglobin single crystal” , PHYSICAL REVIEW LETTERS 87 (15): Art. No. 155501, 2001

D'Angelo P, Benfatto M, Della Longa S, Pavel NV, “Combined XANES and EXAFS analysis of Co2+, Ni2+, and Zn2+ aqueous solutions”, PHYSICAL REVIEW B 66 (6): Art. No. 064209, 2002

Biological applications

Hasnain SS, Hodgson KO, “Structure of metal centres in proteins at subatomic resolution “, JOURNAL OF SYNCHROTRON RADIATION 6: 852-864, 1999

Ascone I, Fourme R, Hasnain SS, “Introductory overview: X-ray absorption spectroscopy and structural genomics”, JOURNAL OF SYNCHROTRON RADIATION 10: 1-3, 2003

Della Longa S, Arcovito A, Benfatto M, Congiu-Castellano A, Girasole M, Hazemann JL, Lo Bosco A," Redox-induced structural dynamics of Fe-heme ligand in myoglobin by x-ray absorption spectroscopy", BIOPHYSICAL JOURNAL 85 (1): 549-558, 2003

Sepulcre F, Proietti MG, Benfatto M, Della Longa S, Garcia J, Padros E, "A quantitative XANES analysis of the calcium high-affinity binding site of the purple membrane", BIOPHYSICAL JOURNAL 87 (1): 513-520, 2004